Zeitschrift: Schweizerische mineralogische und petrographische Mitteilungen = Bulletin suisse de minéralogie et pétrographie

Band: 77 (1997)

Heft: 1

Artikel: Mafic granulites in the Cretaceous sedimentary mélanges from the northern Apennine (Italy) : petrology and tectonic implications

Autor: Montanini, Alessandra

DOI: https://doi.org/10.5169/seals-58469

SCHWEIZ. MINERAL. PETROGR. MITT. 77, 51–72, 1997

Mafic granulites in the Cretaceous sedimentary mélanges from the northern Apennine (Italy): petrology and tectonic implications

by *Alessandra Montanini*[1]

Abstract

The Late Cretaceous ophiolite-bearing mélanges of the External Liguride Units from the northern Apennine are characterized by blocks of mafic and felsic granulite-facies rocks. These granulites are the only record of deep continental basement rocks in the northern Apennine.

The granulite-facies rocks include (1) two-pyroxene granulites, (2) amphibole-rich pyroxene granulites, (3) garnet-bearing pyroxene granulites, (4) pyroxenites and (5) rare felsic granulites. Granulitic assemblages of the mafic rocks consist of plagioclase + clinopyroxene and variable amounts of orthopyroxene, brown amphibole (Ti-rich pargasite), garnet, green spinel, magnetite, ilmenite. Amphibolites formed through retrogression of mafic granulites are quite common. The felsic granulites generally show assemblages made up of quartz + feldspar (mesoperthite) + garnet + rutile, but charnockitic rocks composed of antiperthitic plagioclase + pyroxenes + Fe Ti oxides with or without additional quartz and garnet have been locally found. Most rocks show a retrograde metamorphism closely related to deformations progressively changing from plastic to brittle.

The igneous protoliths of the mafic granulites are interpreted as originated in the deep crust through cumulus of pyroxenes and plagioclase (± olivine) from variably evolved mafic magmas with subalkaline (tholeiitic) affinity. During post-magmatic cooling, subsolidus re-equilibration occurred in granulite-facies conditions (P ~ 7–8 kbar, T ~ 800 °C). Granulite-facies re-equilibration was followed by a retrograde metamorphic evolution from amphibolite- to subgreenschist-facies conditions. Some granulitic rocks have experienced a first retrograde event related to plastic high-T shear zones. Subsequently, a widespread retrograde metamorphism coupled with brittle deformations, overprinted the high-T assemblages. Retrogression to lower temperature conditions is mainly evidenced by growth of amphiboles whose compositional evolution proceeds towards decreasing edenite, tschermakite and Ti-tschermakite substitutions. Replacement of Ti-rich pargasite by low-Ti hornblende or hastingsite characterizes the amphibolitic stage, whereas the change in amphibole composition from hornblende to actinolite records the transition between amphibolite- and greenschist-facies. The extensive hydration caused substantial changes of whole-rock composition (increase of K, Rb, Ba, K/Rb and loss of Ca, Na).

The retrograde metamorphic evolution and the deformations are related to exhumation of the deep crust. It is proposed that the mafic granulites could belong to the deep crust uplifted and sheared during the rifting which led to the opening of the Ligure-Piemontese Basin.

Keywords: granulite-facies, retrograde metamorphism, amphiboles, mineral chemistry, geochemistry, northern Apennine, Ligure-Piemontese Basin.

Introduction

In the northern Apennine, granulite-facies rocks are commonly found as blocks in ophiolite-bearing mélanges of Upper Cretaceous age belonging to the External Liguride Units. It has been reported for a long time that the External Liguride ophiolites (mantle ultramafics and MOR-basalts) are frequently associated with igneous and metamorphic rocks of upper and lower continental crust, i.e. Hercynian granites (MERLA, 1933; EBERHARDT et al., 1962) and mafic granulites (BRAGA et al., 1975). Similar relationships between continental crust and ophiolites have been also de-

[1] Dipartimento di Scienze della Terra, Università degli Studi di Parma, V. delle Scienze 78, I-43100 Parma, Italy. E-mail: ales01@ipruniv.cce.unipr.it.

scribed in some sectors of the Austroalpine domain of the central Alps (e.g. Malenco-Forno nappe, MÜNTENER et al., 1995; MÜNTENER and HERMANN, 1996). A key to the interpretation of this puzzling association may be given by the comparison with the present-day occurrence of continental crustal basement in contact with mantle peridotites in well known settings of ocean-continent transition like the Iberian passive margin (BOILLOT et al., 1995) and the Red Sea (SEYLER and BONATTI, 1988).

The northern Apennine granulitic rocks provide meaningful, although fragmentary, informations about the composition and pre-alpine history of the deep crust in the southern sector of the Adria continental margin, their most likely source-area. Recent geochronological work (MELI et al., 1996) has pointed out that the age of the mafic granulites from the External Liguride Units can be broadly compared with that of deep-seated gabbroic intrusions of Permian age (largely recrystallized in granulite-facies conditions) occurring in the Southalpine and Austroalpine domains (Ivrea Main Gabbro: PIN, 1986; Fedoz gabbro: HANSMANN et al., 1995; Matterhorn-Mt. Collon gabbro: DAL PIAZ et al., 1977) which have been related to the pre-Alpine extensional tectonics (PIN, 1990; DAL PIAZ, 1993).

This paper is aimed to provide a detailed knowledge of petrography, mineralogy, geochemistry and metamorphic history of the granulitic rocks. Based on these data, tectonic implications of their metamorphic evolution and the possible role of the association of granulite-facies rocks and ophiolites belonging to the Jurassic Ligure-Piemontese Basin are discussed. It will be shown that the evolution inferred for the granulitic rocks of northern Apennine can be inserted into the well documented history of passive rifting (e.g. LEMOINE et al., 1987) which led to the opening of the Ligure-Piemontese Basin.

Geological setting

The Liguride Units (Fig. 1a) consist of oceanic rocks (ophiolites and deep sea sediments) of Late Jurassic-Middle Eocene age. They originated from a segment of the Mesozoic Tethys, the Jurassic Ligure-Piemontese Basin (JLPB), and were overthrusted towards NE onto the platform sequences of the Insubrian passive continental margin (Tuscan and Umbro-Marche Units). They are the highest units in the nappe pile of the northern Apennine. According to lithostratigraphic and tectonic features they were subdivided (ELTER and PERTUSATI, 1973) into Internal and External Liguride Units:

1. The Internal Liguride Units Units (IL) are composed of an ophiolitic sequence and their original sedimentary cover of Jurassic-Early Paleocene age (ABBATE et al., 1984). They have been interpreted as fragments of the JLPB oceanic lithosphere which were included into an accretionary prism during Alpine convergence (MARRONI, 1994) and metamorphosed under very low-grade conditions (LEONI et al., 1996). The ophiolitic sequence includes: (i) mantle ultramafic rocks, chiefly represented by depleted lherzolites (RAMPONE et al., 1996); (ii) gabbroic complexes intruded into the mantle rocks and crystallized at intermediate pressure (5–7 kbar, COTTIN, 1984) from primitive basaltic magmas with MORB affinity (HEBERT et al., 1989); (iii) MOR-basalts and sedimentary ophiolitic breccias.

2. The External Liguride Units (EL) consist of turbiditic sequences (Helminthoid flysch) of Upper Cretaceous-Eocene age (ABBATE and SAGRI, 1982) and their "basal complexes" which frequently contain ophiolite-bearing sedimentary mélanges. The origin of these deposits is thought to be related to the transpressive tectonics which affected the EL domain in the Upper Cretaceous (ELTER and MARRONI, 1991). In contrast with the IL, the ophiolites occur exclusively as "slide blocks" (NAYLOR, 1982) or "olistoliths" in the mélanges. The EL units are generally unmetamorphosed, although a very-low grade metamorphic imprint has been found in the westernmost units (i.e. Casanova Complex, VENTURELLI and FREY, 1977). The EL ophiolites are characterized by (i) mantle ultramafics consisting of relatively undepleted lherzolites which have been interpreted as subcontinental mantle (RAMPONE et al., 1995); (ii) sporadic occurrence of gabbroic rocks, (iii) oceanic basalts with N- and T-MORB affinity (VENTURELLI et al., 1981). A peculiar feature of the EL ophiolites is their association with continental crustal rocks. The peridotitic slide-blocks are frequently associated with granulite-facies rocks in the mélanges, although no primary relationships between peridotite and granulitic rocks have ever been found. In contrast, primary contacts between granite slide blocks and ophiolitic basalts can be frequently observed in the Casanova Complex (Fig. 1b) where stretched slices of granitic rocks are either intruded by basaltic dykes or covered by basaltic lava flows and radiolarian cherts (MONTANINI et al., 1995; MOLLI, 1996).

The pre-orogenic features of the External Liguride domain have been inferred only through the nature of the slide-blocks included in the mélanges, i.e. mantle ultramafics, oceanic basalts and continental crustal rocks (MOLLI, 1996). In

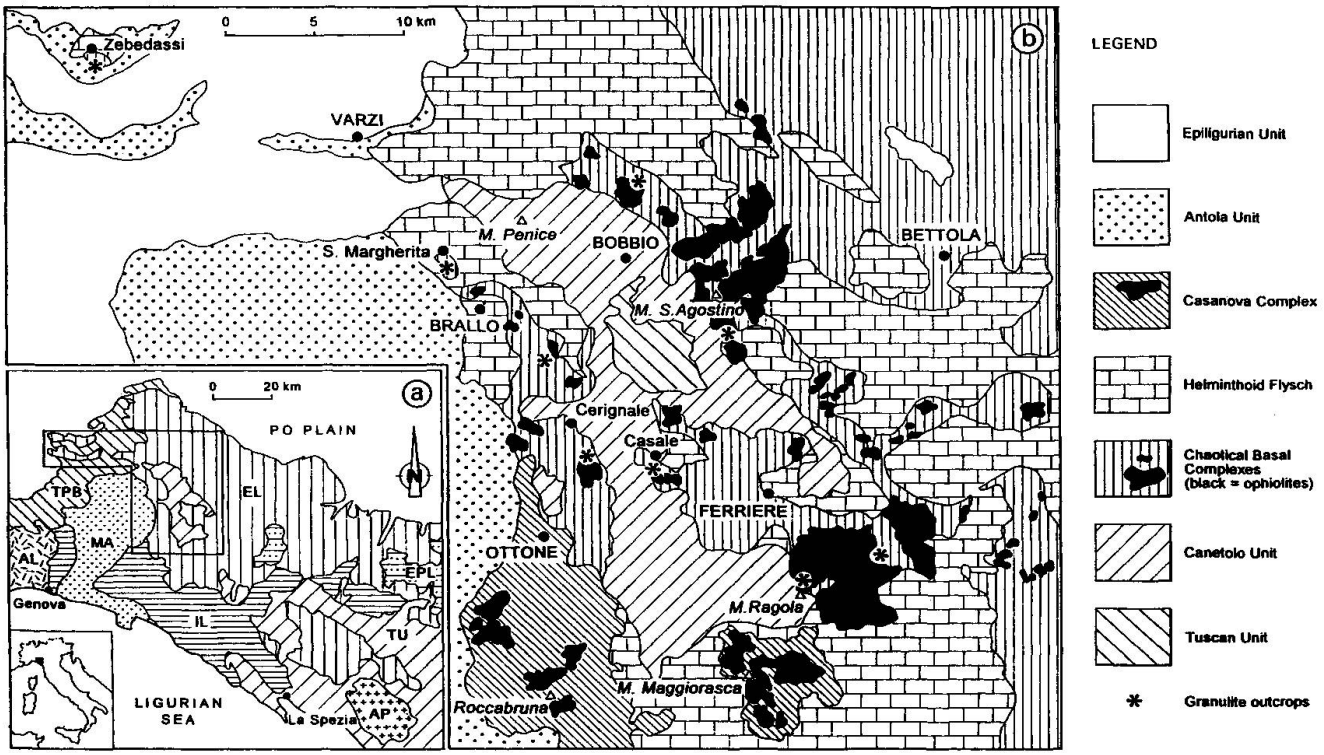

Fig. 1 (a) Tectonic sketch map of the Northern Apennines; abbreviations: AL = Alpine Units, AP = Alpi Apuane Unit, TU = Tuscan and Canetolo Units, MA = Monte Antola Unit, IL = Internal Liguride Units, EL = External Liguride Units, TPB = Tertiary Piemontese Basin, EPL = Epiligurian Units (modified after MOLLI, 1994). (b) Geologic sketch map of the studied area (simplified after "Carta Strutturale dell'Appennino Settentrionale", CNR 1982) and distribution of the main granulite outcrops.

particular, the western part of the EL domain has been considered as the continent-ocean transition between the IL oceanic domain and the thinned continental margin represented by the eastern EL (ZANZUCCHI, 1988; ELTER and MARRONI, 1991); the coupling of continental crust rocks and ophiolites has been related to the Jurassic rifting stage which most probably involved tectonic denudation of the subcontinental mantle (PICCARDO et al., 1992).

Field relations

The distribution of the main outcrops of granulitic rocks is reported in figure 1b. Most of them are hosted in the Mt. Ragola Complex which has been described by MARRONI and TRIBUZIO (1996) and is well exposed in the Mt. Ragola and Casale-Cerignale area (Fig. 1b). Unpublished biostratigraphic data for the sedimentary sequence of this complex give a Santonian-Early Campanian age (MARRONI, pers. comm.). The granulitic rocks may be found as (1) slide blocks and (2) clasts of poligenic clast-supported breccias; other lithologies occurring as blocks in the Mt. Ragola Complex are pyroxenites, peridotites and limestones. The granulitic rocks occurring in the breccias are centimeter- to meter-scale angular or subrounded blocks. Shear zones (millimeter- to meter-scale) are clearly recognizable both in slide blocks and clasts. In the Casale outcrop pluridecametric slide blocks composed of mafic and felsic granulites have been found; these rocks are characterized by a widespread cataclastic fabric along with the occurrence of porphyroclast-free ultracataclastic zones ranging in width from few millimeters to several meters.

Other granulite-bearing mélanges are associated with the large serpentinite bodies of Mt. S. Agostino area and with the minor ophiolitic outcrops of Brallo, S. Margherita and Zebedassi (Fig. 1b). In these localities the granulitic rocks have been found as decimetric clasts of matrix- or clast-supported poligenic breccias resting upon slide blocks of serpentinite (BRAGA et al., 1975). In the westernmost outcrops (Zebedassi, S. Margherita, Fig. 1b) the granulitic rocks are associated with minor clasts of gneisses, micaschists and felsic metavolcanic rocks.

Analytical techniques

Detailed petrographic observations have been carried out on 150 thin sections of granulitic rocks. Mineral analyses were made on 22 selected samples using an electron microprobe JEOL-6400 equipped with TRACOR energy-dispersive microanalytic system; operating conditions were 15 kV accelerating voltage and 0.62 nA probe current. Whole-rock major element analyses have been obtained by XRF on glass disks using the method of FAIRBAIRN and HURLEY (1971); trace elements (Ni, Co, Cr, V, Cu, Zn, Ga, Rb, Sr, Zr, Nb, Y) have been performed by XRF on powder pellets following the correction procedures of LEONI and SAITTA (1976). REE abundances were determined by ICP-MS spectrometry at the laboratory of CRPG (Vandœuvre-les-Nancy).

Petrography

The granulite-facies rocks include different mafic and felsic lithologies which are discussed in detail in table 1. Two-pyroxene mafic granulites are the most frequent rock type; minor anorthosites and pyroxenites have been found as modal variation of the dominant mafic compositions. A common origin for the different types of two-pyroxene granulites is indicated by the occurrence of composite layered rocks.

The mafic rocks consist of plagioclase + pyroxenes ± olivine ± garnet and variable amounts of amphibole and oxides (green hercynitic spinel, ilmenite, magnetite); accessory phases are sulphides, biotite, apatite, zircon. Olivine is likely to be a relic of the original igneous assemblage, whereas garnet originated through subsolidus reaction in the most Fe-rich rocks. The felsic rocks include quartzo-feldspathic granulites (feldspars + quartz + garnet + rutile) and charnockitic rocks (antiperthitic plagioclase ± quartz + pyroxenes ± garnet + Fe–Ti oxides).

The primary magmatic textures of the mafic rocks have not been preserved and the igneous origin of the protoliths can be largely inferred on geochemical grounds (see below). Only one sample of a two-pyroxene granulite (MZ209B) retains large (2–5 mm) subhedral grains of ortho- and clinopyroxene with mutual exsolution lamellae suggesting slow cooling after magmatic crystallization. Different degrees of textural equilibration related to the granulite facies metamorphism can be observed: the mafic granulites range from inequigranular rocks with variable amounts of lobate grain boundaries and 120° triple junctions to equant granoblastic-polygonal. In addition, granulite-facies equilibration yielded two types of subsolidus corona structures:

1. Spinel-pyroxene symplectites in the olivine-bearing rocks at the plagioclase-olivine interface (Fig. 2A); the olivine-plagioclase reaction frequently goes to completion with disappearance of olivine.

2. Garnet (± brown amphibole) as rims or small euhedral grains around clinopyroxene and spinel (Fig. 2B); garnet (± plagioclase ± magnetite) may also be found as exsolution along the clinopyroxene cleavage planes.

Evidence of plastic deformation under granulite-facies conditions is given by (i) the occurrence of weakly deformed mafic rocks showing undulose extinction, bending and kinking in pyroxenes and curved multiple twins in plagioclase; (ii) formation of strongly foliated, protomylonitic to mylonitic microstructures (Fig. 2E–F) where clinopyroxene + Ti-rich brown amphibole recrystallize in pressure shadows of clinopyroxene porphyroclasts; (iii) lobate quartz-feldspar grain boundaries in the felsic granulites. Mylonitic to ultramylonitic zones (extensively modified by low-temperature transformations) also occur in the felsic granulites.

The amphiboles of the mafic granulites have several mode of occurrence which can be summarized as follows: (i) grains with curved grain boundary including hercynitic spinel or Fe–Ti oxides (spinel-rich mafic granulites); (ii) inclusion-free polygonal grains (amphibole-rich pyroxene granulites); (iii) minor constituents of the pyroxene-spinel symplectites, (iv) interstitial grains in contact with garnet (coronas around clinopyroxene in garnet-bearing pyroxene granulites), (v) thin rims between ilmenite and plagioclase (opx-rich mafic granulites), (vi) granulation around clinopyroxene (mafic gneisses and mylonites).

A widespread retrograde metamorphism, from upper amphibolite to subgreenschist conditions, overprints the granulitic assemblages. Retrogression is commonly (but not exclusively) related to deformation changing from plastic to brittle.

Mafic granulites have been locally transformed into *mylonitic amphibolites* consisting of plagioclase + greenish-brown amphibole + ilmenite ± magnetite; clinopyroxene, green spinel and garnet may be present as relics of the granulitic assemblage. They are medium-grained rocks with porphyroclasts of plagioclase and amphibole (sometimes with clinopyroxene cores) into a recrystallized matrix formed by the same minerals along with Fe–Ti oxides.

The subsequent stage of retrogression in both granulites and mylonitic amphibolites is accom-

Tab. 1 Summary of petrographic features of the granulitic rocks.

Rock type	Textural and microstructural features	Assemblage and reaction textures
1 – TWO-PYROXENE GRANULITES		
Opx-rich mafic granulites	Medium-grained rocks. Granoblastic texture with well-developed 120° triple junctions. No preferred orientation of minerals.	*plagioclase + opx + cpx + ilmenite + biotite + greenish-brown amphibole (hastingsitic hornblende) + apatite +zircon.*
Spinel-rich mafic granulites	Medium-grained inequigranular rocks. Curved grain boundaries prevail, although 120° triple junctions are common. Rare occurrence of plagioclase and pyroxene-rich layers. No preferred orientation of minerals clearly recognizable.	*plagioclase + cpx + opx + red-brown amphibole (Ti-rich pargasite) + spinel ± Fe–Ti oxides (ilmenite, magnetite) ± biotite.* Opaques typically enclosed into large amphiboles with curved grain boundaries or rimmed by amphibole.
Mafic gneisses and mylonites	Medium to coarse-grained inequigranular rocks. Curved grain boundaries prevail. Textures ranging from gneissic to protomylonitic and mylonitic. Most of these rocks show aligned clusters of augen-shaped pyroxenes along with undeformed spinel in a highly sheared plagioclase matrix.	*plagioclase + cpx + opx + spinel + brown amphibole (Ti-rich pargasite).* The amphibole (frequently recrystallized) typically occurs as partial replacement of clinopyroxene around the margins or along the cleavage plains. Synkinematic crystallization of cpx + brown amphibole in pressure shadows of clinopyroxene porphyroclasts.
Symplectite-bearing granulites	Medium-grained inequigranular rocks. Microstructure incompletely equilibrated with prevailing curved grain boundaries and opx-spinel simplectitic intergrowths. Rare kinkbands in olivine and pyroxenes. Occurrence of plagioclase and amphibole rich-layers.	*plagioclase + cpx + opx + spinel + brown amphibole (Ti-rich pargasite) + magnetite ± biotite ± sphene ± sulphides.* Coronas consisting of a inner shell of opx-spinel or cpx-spinel symplectites (± small amounts of brown amphibole) and an outer rim of clinopyroxene, occur at the contact between plagioclase and relic igneous olivine (Fo_{77-74})
2 – AMPHIBOLE - RICH PYROXENE GRANULITES	Medium-grained rocks with granoblastic-polygonal equilibrium textures. No preferred orientation of minerals.	*plagioclase + cpx + red-brown amphibole (Ti-rich pargasite) + opaques + apatite.*
3 – GARNET-BEARING PYROXENE GRANULITES	Medium-grained rocks with protomylonitic microstructure (highly strained clinopyroxene showing bending and kinking, along with relatively undeformed garnet + spinel in a sheared plagioclase matrix).	*plagioclase + cpx + garnet + green spinel + brown amphibole + magnetite + ilmenite + sulphides.* Garnet occurring as (i) coronas of clinopyroxene and spinel, (ii) exsolution lamellae into Al-rich clinopyroxene.
4 – PYROXENITES	Medium to coarse-grained inequigranular rocks with abundant triple point grain boundaries. Evidence of shear given by (i) small recrystallized clinopyroxene rimming larger deformed clinopyroxene grains, (ii) thin mylonitic bands.	*cpx + opx + spinel + brown amphibole ± plagioclase.* Amphibole originates along clinopyroxene cleavages or at the contact between clinopyroxene and spinel.
5 – FELSIC GRANULITES	Medium-grained rocks with granoblastic texture, often inequigranular due to garnet and/or antipertithic plagioclase porphyroclasts; lobate grain boundaries between quartz and feldspars in weakly deformed rocks.	Quartzo-feldspathic granulites: *qtz + feldspar (mesoperthites) + garnet ± plagioclase + rutile + apatite + zircon.* Charnockitic rocke: *antiperthitic plagioclase ± qtz + orthopyroxene ± clinopyroxene ± garnet + Fe–Ti oxides ± apatite.*

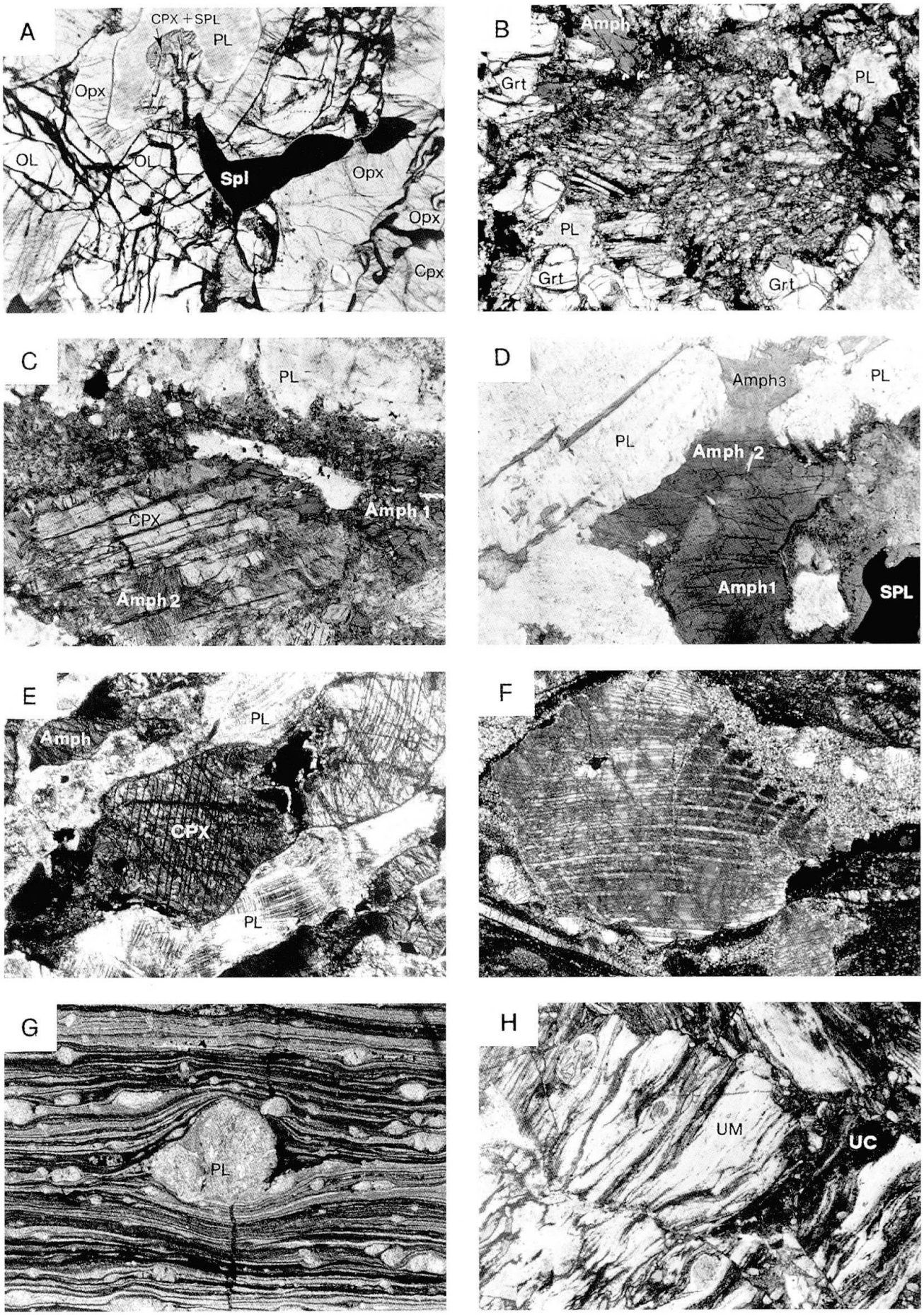
A
CPX + SPL
PL
Opx
OL
OL
Spl
Opx
Opx
Cpx
B
Amph
Grt
PL
PL
Grt
Grt
C
PL
CPX
Amph 1
Amph 2
D
Amph3
PL
PL
Amph 2
Amph1
SPL
E
Amph
PL
CPX
PL
F
G
PL
H
UM
UC

panied by cataclastic deformations clearly postdating ductile deformation and recrystallization. The cataclastic effects range from grain-scale cracking (mainly affecting plagioclase) to pervasive brecciation into centimeter-sized clasts; in places, ultracataclasites overprint already plastically deformed rocks (Fig. 2H).

This cataclastic stage is characterized by growth of green and bluish-green amphibole (± epidote) as (i) aggregates and fibrous crystals within plagioclase, (ii) fibrous rims or epitaxial overgrowths on clinopyroxene and brown amphibole, (iii) filling of veins linking the amphiboles (i) and (ii) (Fig. 2D). Amphiboles with compositions ranging from hornblende to actinolite frequently occur in the same rock as irregular or patchy intergrowths, whereas exsolution of one amphibole from another has never been observed. Other minerals occurring as filling of dilatant cracks are sericite, epidote and chlorite. The veins often cut the foliation defined by the plastic deformations at high angles. Retrograde assemblages are best developed in proximity of the brittle failure zones. The felsic granulites show replacement of the high-grade assemblage by albite + quartz + chlorite + sphene ± actinolite.

Finally, very low-grade assemblages (pumpellyite + actinolite + albite + chlorite ± sericite) have locally developed under static conditions in some mafic granulites.

Mineral chemistry

PYROXENES

The pyroxenes of the mafic granulites (Tab. 2) can be usually classified as aluminian ferroan diopside and aluminian ferroan enstatite according to the recommended IMA nomenclature (ROCK, 1990). Ortho- and clinopyroxene display a continuous variation in Fe/(Mg + Fe) ratios (respectively 0.19–0.41 and 0.08–0.33) giving rise to a considerable enrichment trend in the pyroxene quadrilateral (Fig. 3).

A conspicuous feature of most pyroxenes is the high Al_2O_3 content (up to 8.9 wt% in clinopyroxene and 6.1 wt% in orthopyroxene), which give rise to pronounced Ca-Tschermak and Mg-Tschermak substitutions. Concentrations of TiO_2 in clinopyroxene vary from low (≤ 0.3 wt% in the orthopyroxene- and amphibole-rich pyroxene granulites, analyses 1–2, 5) to moderate (1.2–1.6 wt%) in the other rocks; Na_2O ranges between 0.8 and 1.6 wt%. Chromium is not detectable or low in both clino- and orthopyroxene ($Cr_2O_3 \leq 0.30$ wt%). The low CaO content of orthopyroxene coexisting with clinopyroxene (0.25–0.95 wt%) is typical of slow-cooled pyroxenes of granulites (RIETMEJIER, 1983); a wide field of immiscibility between Ca-poor and Ca-rich pyroxenes, due to subsolidus equilibration, is clearly recognizable in figure 3. The arrangement of the tie-lines in figure 3 indicates recrystallization at equilibrium under the same temperature conditions.

Prominent chemical zoning involving Al_2O_3, FeO, MgO and, to a lesser extent, TiO_2 and Na_2O, can be observed in both pyroxenes. The zoning is developed only in the outer rims of the crystals (within a few tenths of microns) whereas the internal parts are relatively homogeneous. The rims are usually enriched in MgO and depleted in Al_2O_3 and FeO towards the rims (Tab. 2, analyses 1–4, 6–9, 13–16); clinopyroxene sometimes shows rims slightly depleted in TiO_2 and Na_2O. No appreciable Ca zoning can be usually detected in orthopyroxene, whereas the clinopyroxene rims may be enriched in CaO.

FELDSPARS

The plagioclase compositions in most mafic granulites and amphibolites cluster in a narrow range

Fig. 2 Photomicrographs of mafic granulites. Abbreviations: cpx = clinopyroxene; opx = orthopyroxene; pl = plagioclase; ol = olivine; spl = spinel; amph = amphibole; grt = garnet. Field of view = 3.0 × 2.0 mm (A–D), 4.8 × 3.2 mm (E–H). (A) Symplectite-bearing granulite = orthopyroxene rim around plagioclase in contact with olivine and development of cpx-spinel symplectites; plane-polarized light. (B) Garnet-bearing pyroxene granulite = growth of garnet and brown amphibole around a large deformed clinopyroxene grain. Plane-polarized light. (C) Amphibolite = relic of flattened clinopyroxene partially replaced by hastingsitic greenish brown amphibole (Amph1) and fibrous light green amphibole (Amph2). Plane-polarized light. (D) Symplectite-bearing granulite = Ti-rich pargasite (reddish-brown to pale brown: Amph1, Tab. 3, analysis 4) zoned towards a Ti-poorer magnesian hastingsitic hornblende (olive green: Amph2, Tab. 3, analysis 10) which grades into a blue-green magnesio-hornblende (Amph3); this latter occurs also as filling of cracks in plagioclase. Pargasite rims an opaque spinel grain. Plane-polarized light. (E) Mafic gneiss = plastically deformed clinopyroxene, brown amphibole and plagioclase (partially replaced by sericite). Crossed Nicols. (F) Mylonite from mafic granulite = large clinopyroxene porphyroclast with fine-grained tails of recrystallized clinopyroxene + brown amphibole. Crossed nicols. (G) Quartzo-feldspathic granulite = mylonitic fabric with porphyroclasts of quartz and antiperthitic plagioclase. Crossed Nicols. (H) Quartzo-feldspathic granulite = angular clasts of strongly foliated ultramylonite cut by a dark, fine-grained, ultracataclasite. Crossed Nicols.

Tab. 2 Selected analyses of pyroxenes. Total iron as FeO; cpx = clinopyroxene, opx = orthopyroxene, c = core, r = rim, (–) = not detected. Structural formulae on the basis of 6 oxygens; $Al^{IV} = 2 - Si$. Samples: 225C = opx-rich mafic granulite, C4 = amphibole-rich pyroxene granulite, 229E = spinel-rich mafic granulite, 253M = mafic gneiss, 252M-209B = symplectite-bearing granulites (* = pyroxenes from olivine-plagioclase corona reaction), AM1 = garnet-bearing pyroxene granulite, 234F = amphibolite (retrogressed granulite).

	1 225C cpx-c	2 cpx-r	3 opx-c	4 opx-r	5 C4 cpx	6 229E cpx-c	7 cpx-r	8 opx-c	9 opx-r	10 253M cpx	11 252M cpx*	12 opx*	13 209B cpx-c	14 cpx-r	15 opx-c	16 opx-r	17 AM1 cpx	18 234F cpx
SiO_2	50.9	52.7	50.9	52.1	49.4	47.8	48.7	50.9	50.9	48.6	50.5	52.8	49.3	50.8	51.7	53.0	50.0	48.4
TiO_2	0.45	0.27	–	–	0.66	1.25	1.50	–	–	1.22	0.81	0.15	0.81	0.81	0.22	–	1.10	0.92
Al_2O_3	3.30	2.33	1.92	1.80	6.28	8.04	7.58	5.64	4.94	8.29	6.81	4.79	8.08	6.42	5.14	4.57	6.24	8.45
Cr_2O_3	–	–	0.30	–	–	–	–	–	–	–	–	–	–	–	–	–	–	0.04
FeO_{tot}	10.5	8.56	24.6	23.6	9.58	8.28	7.32	19.9	20.4	7.31	5.28	13.7	5.71	4.54	14.7	14.7	7.55	7.39
MnO	–	0.51	.78	0.62	0.25	–	–	0.93	–	0.16	–	0.20	–	–	0.38	–	0.17	0.11
MgO	12.6	13.6	20.8	20.6	11.6	11.8	12.3	22.4	23.0	12.8	14.3	27.8	13.0	14.1	26.8	27.2	12.4	11.9
CaO	20.8	22.1	0.46	0.34	21.4	21.0	21.5	0.34	0.35	19.8	20.6	0.59	21.6	21.6	0.36	0.43	21.8	22.0
Na_2O	1.10	–	–	–	1.09	1.51	0.81	–	–	1.52	0.81	–	1.36	1.59	–	–	0.77	1.09
Total	99.65	100.07	99.76	99.46	100.26	99.68	99.71	100.11	99.59	99.70	99.11	100.03	99.86	99.86	99.30	99.90	100.03	100.30
Si	1.918	1.958	1.930	1.962	1.832	1.791	1.811	1.874	1.882	1.787	1.861	1.886	1.818	1.862	1.871	1.900	1.852	1.795
Ti	0.013	0.008	–	–	0.018	0.035	0.042	–	–	0.034	0.022	0.004	0.022	0.022	0.006	–	0.031	0.025
Al^{IV}	0.082	0.042	0.070	0.038	0.168	0.209	0.189	0.126	0.118	0.213	0.139	0.114	0.172	0.138	0.129	0.100	0.148	0.220
Al^{VI}	0.065	0.060	0.016	0.052	0.107	0.146	0.143	0.119	0.097	0.146	0.157	0.080	0.179	0.139	0.090	0.093	0.125	0.146
Cr	–	–	0.009	–	–	–	–	–	–	–	–	–	–	–	–	–	–	0.001
Fe	0.331	0.266	0.780	0.743	0.297	0.259	0.228	0.613	0.631	0.225	0.163	0.409	0.176	0.139	0.445	0.441	0.234	0.227
Mn	–	0.016	0.025	0.020	0.008	–	–	0.029	–	0.005	–	0.006	–	–	0.012	–	0.005	0.003
Mg	0.708	0.753	1.175	1.179	0.641	0.659	0.682	1.229	1.268	0.701	0.785	1.480	0.714	0.770	1.446	1.453	0.685	0.652
Ca	0.840	0.880	0.019	0.014	0.850	0.843	0.857	0.013	0.014	0.780	0.813	0.023	0.853	0.848	0.014	0.017	0.865	0.867
Na	0.080	–	–	–	0.078	0.110	0.058	–	–	0.108	0.058	–	0.097	0.113	–	–	0.055	0.078

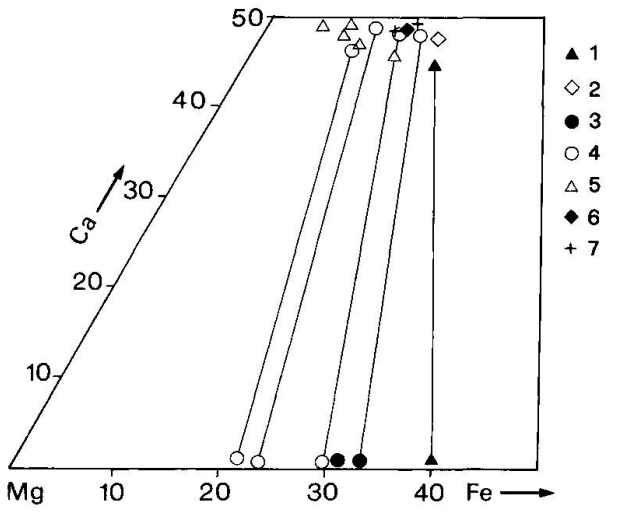

Fig. 3 Composition of the pyroxenes from the mafic granulites. Symbols: 1 = opx-rich mafic granulite, 2 = amphibole-rich pyroxene granulite, 3 = spinel-rich mafic granulite, 4 = symplectite-bearing granulite, 5 = mafic gneiss, 6 = garnet-bearing pyroxene granulite, 7 = relic pyroxenes in the amphibolites.

between An_{52} and An_{47}; the Or content is always low ($K_2O \leq 0.3$ wt%). A distinct reverse zoning (with cores enriched in Na_2O and outer rims depleted in CaO and Al_2O_3) is recognizable in the rocks showing well preserved plagioclase with no retrograde alteration to sericite. For instance, the plagioclase composition in the sample MZ229E varies from An_{59} in the core to An_{67} in the rim; similarly, the plagioclase of an orthopyroxene-rich granulite (sample 225C) ranges between An_{47} an An_{59}.

The appearance of albite (+ sericite ± pumpellyite ± quartz) in the mafic granulites showing extensive retrogression is rare.

The feldspars occurring in the quartzo-feldspathic granulites are mesoperthites composed of K-feldspar, albite and Ba-rich alkalifeldspar (up to 7.2 wt%), whereas the charnockitic rocks contain relatively sodic plagioclase (An_{38-28}) with exsolved blebs of K-feldspar.

AMPHIBOLES

Twenty selected analyses of amphiboles occurring in the mafic granulites are reported in table 3. They are calcic amphiboles spanning a wide range of compositions from Ti- and alkali-rich (pargasite, ferroan pargasite and magnesio-hastingsite) to Ti-free and alkali-poor amphiboles belonging to the actinolite-tremolite series.

The brown and greenish-brown amphiboles of the primary granulitic assemblage (analyses 1–9) are Ti-rich pargasite and hastingsite showing a wide range of TiO_2 (1.83–4.15 wt%), Na_2O (1.66–3.80 wt%) and K_2O (0.60–2.18 wt%) contents; Na^A and K^A show a rough negative correlation. The large variations of $(K/Na)^A$ are largely dependent on bulk-rock chemistry, whereas the highly variable TiO_2 is probably controlled by coexistence or lack of a Ti-phase. The high values of TiO_2 and alkalis are typical of amphiboles from granulitic terrains (RAASE, 1974; GLASSLEY and SORENSEN, 1980; RAASE et al., 1986), because the Ti-tschermakite substitution is favoured by high temperatures (SPEAR, 1981).

The brown-green amphiboles of the mylonitic amphibolites (analysis 11–13) or those rimming Ti-richer pargasite in the mafic granulite (analysis 10, Fig. 2D) are relatively low-Ti hastingsitic amphiboles.

The bluish-green, green to colorless amphiboles vary from hornblende to actinolite (analyses 15–20, Tab. 3). The transition from hornblende to actinolite is marked by gradually decreasing concentrations of TiO_2 (1.0–0 wt%), Al_2O_3 (10.7–1.9 wt%) and Na_2O (2.10–0.22 wt%), with no compositional gap. K_2O is always very low (0.2 wt%). Small amounts of chlorine (commonly not detectable in pargasite and hornblende) have been found in the actinolitic amphiboles (Cl = 0.1–0.2 wt%). The general trends of the amphiboles (Fig. 4) are towards an increase of Si and a decrease of Ti, alkalis and Al, although a considerable scatter may occur as a consequence of different whole-rock compositions. In particular, the variations can be described in terms of decreasing pargasite ($(Na + K)^A + 2Al^{IV} + Al^{VI} \Leftrightarrow (Fe^{2+}, Mg)$, Si), tschermakite ($(Al^{VI} + Fe^{3+}) + Al^{IV} \Leftrightarrow Mg$, Si) and Ti-tschermakite ($Ti, 2Al^{IV} \Leftrightarrow Mg, 2Si$) substitutions. In contrast, Na^{M4} is not correlated with Ca, Si and Al^{IV}, which rules out any significant role for the glaucophane substitution.

The $Mg/(Mg + Fe^{2+})$ ratios of the amphiboles ratios range between 0.59 and 0.94; this high variability is only slightly enhanced by the large uncertainty in the Fe^{2+} and Fe^{3+} recalculation, since the ratio Mg/(Mg + Fe) calculated assuming total iron as FeO varies between 0.56 and 0.86.

OXIDES

The oxides of the primary granulitic assemblage include green hercynitic spinel (analyses 5–10, Tab. 4), ilmenite (analyses 1, 3) and magnetite (analysis 4). Retrograde reactions involving breakdown of Ti-rich amphiboles yield ilmenite (amphibolite 234F, analysis 2), which in turn is replaced by sphene + magnetite. Green spinel has very low Cr contents ($Cr_2O_3 < 1$ wt%) and vari-

Tab. 3 Selected analyses of amphiboles. Structural formulae on the basis of 23 oxygens. Fe^{3+} and Fe^{2+} recalculated following SPEAR and KIMBALL (1984), assuming M4 and A sites occupied only by Ca, Na, K and Σ(cations) – (Ca + Na + K) = 13. Classification according to LEAKE (1978): P = pargasite, FP = ferroan pargasite, MHA = magnesio-hastingsite, MHAH = magnesian hastingsitic hornblende, MH = magnesio-hornblende, AH = actinolitic hornblende, TH = tremolitic hornblende, A = actinolite. Samples: 229E = spinel-rich mafic granulite, 209B-201A = symplectite-bearing granulite, C4 = amphibole-rich pyroxene granulite, D828, AM1 = garnet-bearing pyroxene granulite granulite, 225C = opx-rich mafic granulite, 253M-2074H = mafic gneisses, 234F-D838 = amphibolites, AM5 = strongly retrogressed mafic granulite.

	Granulite-facies amphiboles									Retrograde amphiboles										
	1	2	3	4	5	6	7	8	9	10	11	12	13	14	15	16	17	18	19	20
	229E	209B	209B	201A	C4	D828	AM1	225C	253M	201A	234F	234F	D838	201A	2074H	201A	253M	234F	AM5	AM5
	FP	P	P	FP	FP	P	FP	MHAH	P	MHAH	FP	MHA	MHA	MH	TH	MH	MH	AH	AH	A
SiO_2	40.4	40.6	40.3	41.0	39.8	41.1	41.0	43.0	41.4	44.6	41.4	40.6	41.5	48.5	53.3	48.5	51.6	51.4	51.9	54.9
Al_2O_3	14.7	16.2	15.6	15.4	14.9	14.6	15.7	11.9	14.8	10.9	15.2	13.3	15.6	8.57	5.46	8.57	6.30	5.32	4.19	1.43
TiO_2	3.56	2.26	4.15	3.17	3.47	3.32	2.62	1.83	2.80	0.79	2.41	2.93	1.39	0.20	–	0.20	0.18	0.28	0.34	–
MgO	11.4	14.5	13.2	11.9	10.6	12.2	12.1	12.4	13.7	12.4	11.8	10.9	13.0	14.0	19.8	14.0	17.9	16.4	12.9	16.2
FeO	12.6	9.25	9.45	11.8	13.8	12.0	11.6	14.0	10.2	15.1	12.9	15.5	12.2	13.8	5.96	13.8	8.80	11.0	17.3	13.6
MnO	0.11	0.19	0.18	–	0.32	0.48	–	0.20	–	0.19	0.15	0.28	–	0.25	–	0.25	0.26	–	0.58	0.36
CaO	11.3	11.4	11.2	11.4	11.4	11.5	11.6	11.8	11.7	12.0	11.8	12.2	11.0	11.5	12.2	11.5	11.1	12.5	10.6	10.8
Na_2O	2.14	3.8	3.47	2.14	2.76	2.44	2.84	1.66	2.91	1.90	2.61	2.48	3.26	1.42	1.14	1.42	1.66	1.61	0.73	0.24
K_2O	1.85	0.76	0.77	1.65	1.50	0.53	0.70	1.61	0.70	0.31	0.14	0.22	0.56	0.14	–	0.14	–	0.10	–	0.06
Total	98.06	98.96	98.32	98.46	98.55	98.17	98.16	98.40	98.21	98.19	98.41	98.41	98.51	98.38	98.08	98.38	97.80	98.61	98.54	97.82
Si	5.966	5.806	5.851	5.979	5.907	5.974	5.974	6.298	5.987	6.492	6.004	6.003	5.960	6.900	7.339	6.900	7.181	7.301	7.482	7.871
Al^{IV}	2.034	2.194	2.149	2.021	2.093	2.026	2.026	1.702	2.013	1.508	1.996	1.997	2.040	1.100	0.661	1.100	0.819	0.699	0.518	0.129
Al^{VI}	0.526	0.537	0.521	0.627	0.515	0.476	0.672	0.352	0.510	0.362	0.603	0.321	0.602	0.338	0.225	0.338	0.214	0.192	0.194	0.113
Ti	0.395	0.243	0.453	0.348	0.387	0.363	0.287	0.202	0.305	0.086	0.263	0.326	0.150	0.021	–	0.021	0.019	0.030	0.037	0.025
Fe^{3+}	0.180	0.484	0.117	0.224	0.099	0.455	0.225	0.471	0.324	0.636	0.439	0.407	0.741	0.795	0.532	0.795	0.810	0.181	0.455	0.022
Mg	2.509	3.090	2.856	2.586	2.345	2.643	2.628	2.707	2.952	2.690	2.551	2.402	2.783	2.969	4.063	2.969	3.712	3.472	2.771	3.462
Fe^{2+}	1.376	0.622	1.030	1.215	1.614	1.003	1.189	1.244	0.909	1.202	1.126	1.510	0.724	0.847	0.154	0.847	0.215	1.126	1.631	1.609
Mn	0.014	0.023	0.022	–	0.040	0.059	–	0.025	–	0.023	0.018	0.035	–	0.030	0.026	0.030	0.031	–	0.071	0.044
Ca	1.788	1.747	1.742	1.781	1.813	1.791	1.811	1.852	1.813	1.872	1.834	1.933	1.693	1.753	1.80	1.753	1.655	1.902	1.645	1.659
Na^{M4}	0.212	0.253	0.258	0.219	0.187	0.209	0.189	0.148	0.187	0.128	0.166	0.067	0.307	0.247	0.200	0.247	0.345	0.098	0.204	0.067
Na^{A}	0.401	0.801	0.719	0.386	0.607	0.479	0.614	0.323	0.629	0.408	0.568	0.644	0.601	0.145	0.104	0.145	0.103	0.346	–	–
K	0.349	0.139	0.143	0.307	0.284	0.098	–	0.301	0.129	0.058	0.026	0.041	0.103	0.025	–	0.025	–	0.018	0.130	0.011
Sum-A	0.749	0.940	0.862	0.693	0.891	0.577	–	0.624	0.758	0.465	0.594	0.685	0.703	0.170	0.104	0.170	0.103	0.364	–	0.744

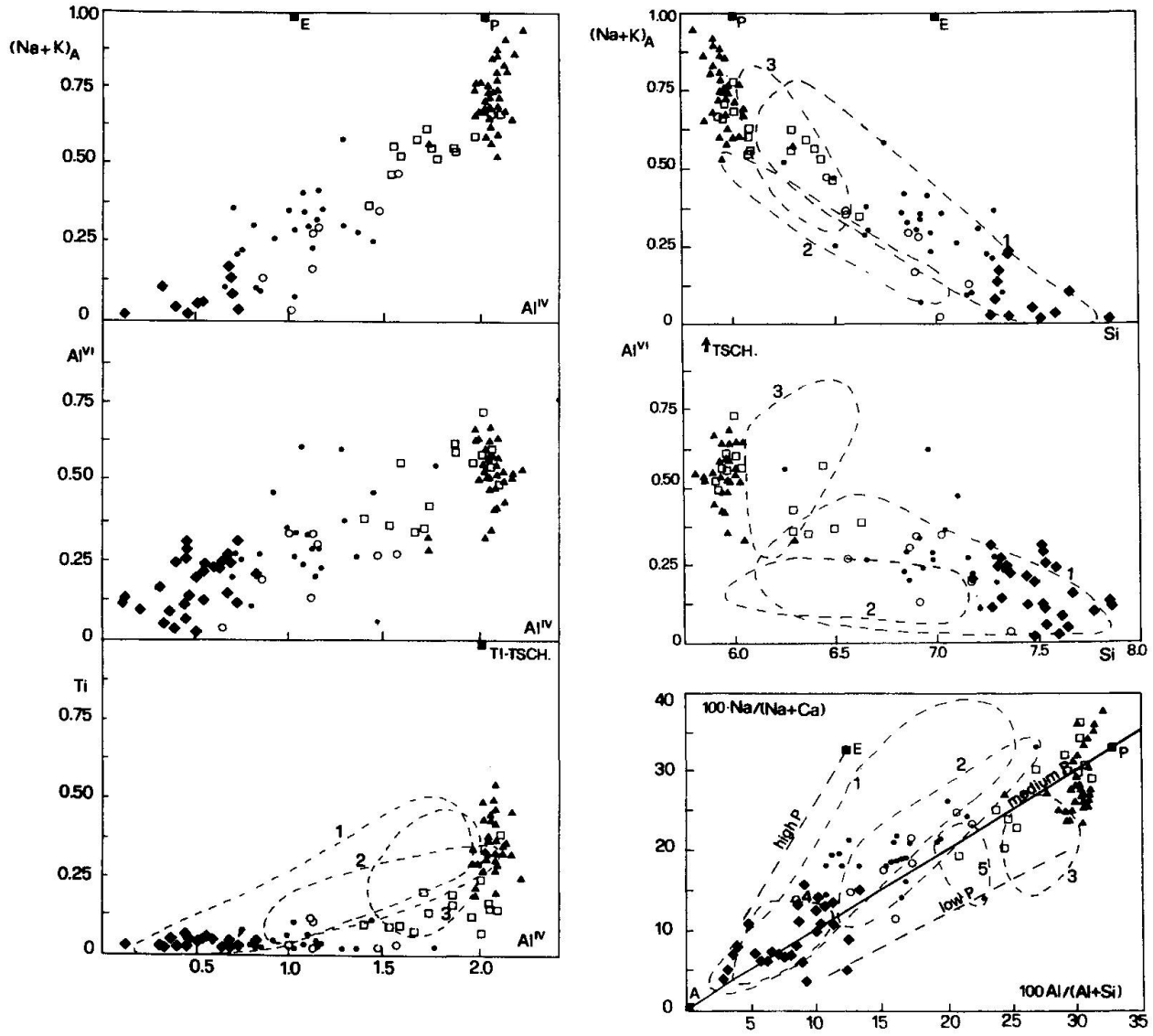

Fig. 4 Compositional variations of the amphiboles. P = pargasite, E = edenite, TSCH = tschermakite, TI-TSCH = Ti-tschermakite. Granulite facies amphiboles = brown Ti-rich pargasitic amphiboles (▲). Retrograde amphiboles = hastingsitic amphiboles replacing clinopyroxene (□), green and blue-green hornblende as replacement of clinopyroxene and brown amphibole (●), blue-green hornblende from veins (○), pale green actinolitic amphiboles (◆). The reported fields include the amphiboles from ophiolitic gabbros (1 = Northern Apennines, CORTESOGNO and LUCCHETTI, 1984; 2 = Chenaillet Massif, Western Alps, MEVEL et al., 1978) and from the Ivrea zone mafic granulites (3 = undeformed rocks, CAPEDRI, 1971; 4 and 5 = low- and medium-T shear zones, BRODIE and RUTTER, 1985). Trends for amphiboles from high-, medium- and low-P regional metamorphic terrains after LAIRD and ALBEE (1981).

able Mg/(Mg + Fe^{2+}) ratios depending on the whole-rock composition.

GARNET

The garnets of the mafic granulites are pyrope-almandine-grossular-solid solutions (Py = 37.0–28.1 mole %, Alm = 42.4–48.8 mole %, Gr = 12.7–22.2 mole %). The garnets analyzed in felsic granulites are grossular-poor and have a much higher almandine content. Representative analyses (1–3) are reported in table 5. All the garnets have low to negligible spessartine content (≤ 3.2 mole %).

Most garnets of both mafic and felsic granulites do not show appreciable zoning. A slight decrease in pyrope (37.0–34.7 mole %) with a corresponding increase in almandine (43.2–45.6 mole %) and grossular (12.7–16.4 mole %) can be sometimes observed from core to rim in the mafic granulites. This is probably due to diffusion during retrograde evolution.

Tab. 4 Selected analyses of Fe–Ti oxides. Il = ilmenite, Mag = magnetite, Spl = hercynitic spinel. Fe_2O_3 calculated normalizing formulae to $\Sigma R3 = Ti + Al + Cr + Fe^{3+} = 1$ for ilmenite and $\Sigma R2 = 1$, $\Sigma R3 = 2$ for spinel and magnetite. (–) = not detected. Samples: 225C = opx-rich mafic granulite, 234F = amphibolite, 229E-T125 = spinel-rich mafic granulites, 2074H = mafic gneiss, 252M = symplectite-bearing granulite, AM1 = garnet-bearing pyroxene granulite.

	1 225C Ilm	2 234P Ilm	3 229E Ilm	4 229E Mag	5 229E Spl	7 T125 Spl	8 2074H Spl	9 252M Spl	10 AMI Spl
TiO_2	45.4	49.5	51.6	5.15	0.12	–	–	–	–
Al_2O_3	–	0.14	0.17	1.90	58.0	65.4	64.5	63.0	51.0
Cr_2O_3	–	–	–	–	0.27	0.76	0.87	0.17	–
Fe_2O_3	5.48	3.09	1.12	57.6	5.72	2.85	0.73	2.22	14.2
FeO	46.6	45.2	44.8	35.7	26.0	10.2	16.4	18.4	26.7
MnO	1.03	1.92	2.62	0.22	0.43	–	–	–	–
MgO	0.34	1.02	0.46	0.32	9.77	20.9	16.7	15.2	8.96
Total	98.82	100.87	100.77	100.89	100.31	100.11	99.20	98.99	100.86
Ti	0.909	0.937	0.974	0.145	0.002	–	–	–	–
Al	–	0.004	0.005	0.084	1.871	1.931	1.968	1.952	1.691
Cr	–	–	–	–	0.006	0.015	0.018	0.004	–
Fe^{3+}	0.108	0.059	0.021	1.626	0.118	0.054	0.014	0.044	0.301
Fe^{2+}	1.030	0.952	0.94	1.120	0.594	0.214	0.356	0.405	0.628
Mn	0.023	0.041	0.056	0.007	0.010	–	–	–	–
Mg	0.013	0.038–	0.017	0.018	0.398	0.780	0.644	0.595	0.376

Tab. 5 Selected analyses of garnet, micas, epidote, pumpellyite. Grt = garnet (1 = rim of clinopyroxene; 2–3 = cores of unzoned grains), Bt = biotite, Ms = fine-grained muscovite (sericite), Ep = epidote, Pmp = pumpellyite, Chl = chlorite. (–) = not detected. Structural formulae of garnet calculated on basis of 12 O ($\Sigma R2 = Ti + Al + Cr + Fe^{3+} = 2$). Structural formulae of hydrous minerals normalized to O = 11 for micas, O = 25 for epidote (total iron as Fe_2O_3), O = 49 for pumpellyite ($\Sigma R3 = Ti + Al + Cr + Fe^{3+} = 10$), O = 14 for chlorite (assuming all iron is ferrous). Samples: D828-AM1 = garnet-bearing pyroxene granulites, L12 = quartzo-feldspathic granulite, 225C-AM12 = opx-rich granulite (AM12 strongly retrogressed), 2374 = mafic gneiss, D838-234F = amphibolites, 201A = symplectite-bearing granulite, C4 = amphibole-rich pyroxene granulite.

	1 D828 Grt	2 AM1 Grt	3 L12 Grt	4 225C Bt	5 D838 Ms	6 2374 Ms	7 234F Ep	8 234F Ep	9 201A Ep	10 2374 Pmp	11 234F Chl	12 C4 Chl	13 253M Chl	14 AM12 Chl
SiO_2	39.2	39.2	38.6	37.5	50.4	47.6	38.4	38.4	38.9	38.4	26.2	29.4	30.2	33.8
TiO_2	–	–	–	6.01	–	–	–	–	–	0.27	–	–	–	–
Al_2O_3	22.1	22.8	22.8	14.0	28.7	34.8	26.5	24.8	30.0	27.3	20.1	17.1	15.8	12.6
Cr_2O_3	0.20	–	–	–	–	–	–	–	–	–	–	–	–	–
Fe_2O_3	–	–	–	–	–	–	9.96	12.8	6.81	–	–	–	–	–
FeO	21.5	21.4	25.7	12.6	2.02	0.31	–	–	–	1.22	28.8	22.3	21.6	18.0
MnO	0.88	0.72	0.46	–	–	0.22	0.28	0.14	–	–	0.3	0.2	–	0.23
MgO	8.81	8.73	10.7	16.0	2.82	0.57	–	–	0.12	3.48	13.3	18.9	21.7	24.7
CaO	6.97	7.33	0.92	–	–	0.39	23.4	22.8	23.3	22.8	0.2	–	–	0.11
Na_2O	–	–	–	–	–	1.35	–	–	–	–	–	–	–	–
K_2O	–	–	–	10.1	11.2	10.3	–	–	–	–	–	–	–	–
Total	99.66	100.18	99.18	96.21	95.14	95.54	98.54	98.94	99.24	93.96	88.9	88.1	89.30	89.44
Si	2.995	2.975	2.963	2.825	3.355	3.176	6.014	5.992	5.935	12.016	2.71	3.018	3.047	3.331
Ti	–	–	–	0.341	–	–	–	–	–	0.064	–	–	–	–
Al^{IV}	–	–	0.037	1.175	0.645	0.824	–	–	–	–	1.229	0.982	0.953	0.669
Al^{VI}	1.991	2.040	2.026	0.069	1.608	1.914	4.579	4.875	5.396	–	1.276	1.087	0.926	0.795
Cr	0.002	–	–	–	–	–	–	–	–	10.071	–	–	–	–
Fe^{3+}	1.372	1.359	–	–	–	–	1.506	1.169	0.782	–	–	–	–	–
Fe^{2+}	0.002	–	1.650	0.794	0.112	0.017	–	–	–	0.319	2.547	1.914	1.823	1.484
Mn	0.057	0.046	0.050	–	–	0.012	0.019	0.037	–	–	0.034	0.023	–	0.019
Mg	1.003	0.988	1.224	1.797	0.280	0.057	–	–	0.027	1.623	2.096	2.891	3.263	3.628
Ca	0.571	0.596	0.076	–	–	0.028	3.826	3.912	3.809	7.644	0.024	–	–	0.012
Na	–	–	–	–	–	0.175	–	–	–	–	–	–	–	–
K				0.971	0.951	0.877	–	–	–	–	–	–	–	–

MICAS

Biotite is an uncommon mineral in mafic granulites. The analyzed biotites have relatively high TiO_2 content and show $Mg/(Mg + Fe^{2+})$ ratios comparable with bulk-rock ratio (e.g. biotite from the sample 225C, Tab. 5 which has $Mg/(Mg + Fe^{2+}) = 0.69$ identical to the whole-rock ratio reported in Tab. 6).

Fine-grained muscovite (sericite) usually forms as replacement of plagioclase (analyses 6,7, Tab. 5). Small amounts of sericite (analysis 5) can also occur together with actinolitic hornblende ± opaque minerals as reaction rims between Ti- and K-rich pargasite and green hercynitic spinel. A moderate phengitic substitution ($(Mg, Fe^{2+})^{VI}Si^{IV} \Leftrightarrow Al^{VI}Al^{IV}$) is frequently observed (FeO up to 2.0 wt%, MgO up to 2.8 wt%; Si = 3.014–3.390 atoms p.f.u.).

EPIDOTE

The epidote occurring as filling of veins (e.g. analysis 9, Tab. 5) can be classified as Fe-epidote ($x_{Ps} = Fe^{3+}/(Fe^{3+} + Al) = 0.25$) according to the compositional subdivision of HOLDAWAY (1972), whereas those replacing clinopyroxene along with magnesio-hornblende are Al-epidote (analyses 7, 10, x_{Ps} respectively 0.19 and 0.13). The coexisting amphibole has a relatively low TiO_2 content (0.5–0.8 wt%). Formation of epidote + hornblende after clinopyroxene instead of hornblende alone is probably controlled by f_{O_2} conditions (LIOU et al., 1974).

CHLORITES

The analyzed chlorites (some of which are reported in Tab. 5) span a wide compositional range between clinochlore and chamosite. A rough positive correlation between Al^{IV} and Al^{IV} is related to decreasing amounts of combined Al^{VI} and Tschermak substitution (TK substitution according to LAIRD, 1988) from the sample 234F (mylonitic amphibolite) to the sample AM12 (strongly retrogressed granulite); a simultaneous increase of Si can be observed in the same direction (Si = 2.57–3.43). Most chlorites fall in the fields of low-grade pumpellyite-bearing rocks (LAIRD, 1988), excluding those from the amphibolite 234F which could have originated in the lower amphibolite facies. The reported trend can be only tentatively attributed to decreasing metamorphic grade as proposed by MARUYAMA et al. (1983), because the dependence of chlorite composition from the metamorphic grade is not well understood (LAIRD, 1988) and the chemistry of chlorites may be also controlled by the composition of the replaced mineral.

P-T conditions of the granulite-facies metamorphism

Two-pyroxene thermometry have been applied to seven samples of mafic granulites using the method of WELLS (1977); only the core compositions of adjacent clinopyroxene-orthopyroxene pairs were employed for the calculations. The more recent pyroxene thermometer of LINDSLEY (1983) cannot be successfully applied to these rocks because of large amounts of non-quadrilateral components (Wo + En + Fs is usually well below 90%). The obtained mean temperature (810 ± 40 °C) is common to many known granulite-facies rocks (BOHLEN, 1987). However, the interpretation of these results cannot disregard the zoning shown by most pyroxenes. Although the zoning seemingly affects only the rims of the pyroxene grains, it cannot be excluded that some kind of compositional readjustement due to high-T diffusion have also changed the core compositions. So, the obtained clinopyroxene-orthopyroxene temperatures do not necessarily correspond to the peak of granulite metamorphism and give only minimum estimate of the thermal conditions of granulite-facies equilibration.

Magnetite-ilmenite thermometry (SPENCER and LINDSLEY, 1981) calculated for coarse-grained intergrowth textures (sample 229E, analyses 3–4 in Tab. 4) gives a T of 590 °C, inconsistent with the mean opx-cpx estimate for the same sample (795 °C), but very close to those calculated by OLIVER (1978) and ELLIS and GREEN (1985) for oxide pairs in mafic granulites. This is in agreement with the notion that in slowly cooled rocks Fe–Ti oxide thermometry only records closing temperatures since the opaque minerals have a closure temperature much lower than the silicate minerals (HARLEY, 1989).

Accurate geobarometry of the mafic granulites is not possible because of the general lack of suitable mineral assemblages. The felsic granulites contain the relevant assemblage garnet-orthopyroxene-plagioclase-quartz but show extensive replacement of orthopyroxene by chlorite, whereas the orthopyroxene is preserved only in garnet-free rocks. In the mafic garnet granulites, the involvement of Fe–Ti oxides in the garnet-forming reaction prevents the formation of quartz, thus excluding the employment of the common geobarometers for mafic garnet-bearing granulites. It

must be noted that the appearance of garnet in some mafic granulites does not necessarily indicate equilibration at higher P than garnet-free rocks: it is widely accepted that garnet formation at constant P is favoured by low mg-ratios of the bulk rock (DE WAARD, 1965; GREEN and RINGWOOD, 1967; MANNA and SEN, 1974; BINGEN et al., 1984) and the garnet granulite AM1 (Tab. 6) has one of the lowest mg-values among the analyzed rocks.

However, a rough pressure constraint can be inferred from the occurrence of the corona reaction between olivine and plagioclase (Fig. 2a) in the symplectite-bearing granulites. Employing the curve of JOHNSON and ESSENE (1982) for the univariant olivine-out reaction in the CMAS system (Fo + An = En + Di + Sp) and the range of two-pyroxene temperatures calculated for the these rocks (780–850 °C), the olivine-plagioclase reaction could have occurred at P ~ 7–8 kbar. The geobarometer of GASPARIK (1987) based on the anorthite content of plagioclase in the assemblage clinopyroxene + orthopyroxene + forsterite + spinel + plagioclase (NCMAS system) gives consistent values (~ 8 kbar) in the same temperature range for An = 48–53 mole %. It must be noted that the actual pressure could be slightly lower, because the curve of JOHNSON and ESSENE (1982) and the calibration of GASPARIK (1987) have been obtained for iron-free systems.

The occurrence of the olivine-plagioclase reaction leading to pyroxene-spinel symplectitic intergrowths is commonly attributed to near-isobaric cooling of mafic igneous rocks under granulite-facies conditions (GRIFFIN and HEIER, 1973; MALL and SHARMA, 1988; BALLHAUS and BERRY, 1991). A stage of near-isobaric cooling after emplacement in the lower crust can be therefore qualitatively deduced for the symplectite-bearing granulites (and interlayered rocks). A similar P-T evolution can be also inferred for the garnet granulites from the occurrence of garnet as thin exsolution lamellae into clinopyroxene: the solubility of alumina in clinopyroxene (which can be expressed through the equilibrium $Ca_2MgAl_2Si_3O_{12} = CaMgSi_2O_6 + CaAlSi_2O_6$) is strongly temperature dependent (HERZBERG, 1978, Fig. 7), so that cooling at near constant pressure may give rise to garnet exsolution in Al-rich clinopyroxenes originated at high temperature (see also GRIFFIN et al., 1984; ELLIS and GREEN, 1985).

In addition, both pressure and temperature decrease are recorded in all the mafic granulites by the ubiquitous Al depletion of the pyroxene rims coupled with a complementary zoning of the plagioclase (KUSHIRO and YODER, 1966; see also LOOCK et al., 1990 for a detailed discussion). Although no inference about the relative chronology of isobaric cooling and decompression can be made, it is conceivable that zoning of pyroxenes and plagioclase could have originated during the first stages of retrograde evolution related to exhumation.

Geochemistry

Bulk rock chemical analyses of 19 mafic granulites and amphibolites are presented in table 6; REE abundances determined on relatively fresh samples are reported in table 7.

The mafic rocks display a wide range of mg-values (100 $Mg/(Mg + Fe^{2+})$ = 56–83) which show rough correlations with several elements (e.g. positive for Ni and negative for TiO_2, MnO, V, Zn, Y, ΣREE, Fig. 5, Tab. 6–7). These chemical variations argue for a magmatic origin with a differentiation trend from Mg-rich to Fe-rich compositions; this is also indicated by the projection in the conventional AFM diagram.

The major element compositions (e.g. high Al_2O_3 contents, mostly ranging between 19 and 22 wt%) do not match those of natural basaltic melts. The very low contents of incompatible elements which are currently considered as immobile (Zr, Nb, Y, P) strongly suggest that the igneous protoliths of the mafic granulites were mafic igneous rocks of cumulus origin with negligible amounts of trapped melt. The abundance of incompatible elements in cumulitic rocks is controlled by the degree of fractionation and the amount of trapped liquid, but their ratios reflect those of the parental melts if the values of bulk crystal/liquid partition coefficient are similar. The ratios Zr/Nb (4.8–11.3), Y/Nb (1.6–8.3) and Zr/Y (0.62–2.92) of the mafic rocks fall in the range observed for subalkaline basaltic liquids; it should be noted that the relatively wide range of Zr/Nb and Y/Nb could be due to the scarce analytical accuracy for Nb at low concentrations (Tab. 6) more than to a real scatter of these ratios in the parental liquids.

Ni is generally low, excluding the olivine-bearing rocks (analyses 12–14, Tab. 6) and the mafic gneiss 258M (analysis 9), which also show the highest Co and Cr contents. It is likely that these rocks represent cumulates originated from the most primitive melts where olivine was the liquidus phase.

Relatively slight Eu depletion or no Eu anomaly occur in the most REE-enriched sample C4 and in the sample 229E (Fig. 6, patterns 1–2), whereas increasing positive Eu anomalies are observed in the other rocks. Ce, Sm and Nd enrich-

Tab. 6 Chemical analysis of selected mafic granulites. Total iron as Fe_2O_3; mgV = 100 Mg/(Mg + Fe^{2+}) ratio calculated assuming Fe_2O_3/FeO = 0.15. Samples: 1–4 = opx-rich granulites; 5 = amphibole-rich pyroxene granulite; 6–8 = spinel-rich granulites; 9–11 = mafic gneisses; 12–14 = symplectite-bearing granulites; 15 = garnet-bearing pyroxene granulites; 16–18 = amphibolites; 19 = strongly retrogressed mafic granulite. ( ) = less accurate values. (–) = not determined, n.d. = not detected ; detection limit for Nb and Y = 3 ppm.

	1 225C	2 237H	3 AM22	4 AM12	5 C4	6 229E	7 223B	8 239H	9 258M	10 253M	11 235G	12 209B	13 259M	14 201A	15 AM1	16 234F	17 AM6	18 AM2	19 AM5
SiO_2	46.9	42.8	42.5	46.8	43.7	41.3	45.7	44.7	42.5	45.3	48.3	43.8	43.4	47.4	43.2	39.6	44.5	43.7	44.3
TiO_2	0.80	1.88	1.07	1.04	1.38	1.33	1.18	0.51	0.45	0.56	0.46	0.28	1.56	0.55	1.08	1.56	0.63	0.94	1.43
Al_2O_3	21.7	19.7	21.7	20.6	20.6	22.3	20.9	23.4	13.6	20.4	19.9	20.2	17.1	22.2	21.7	21.6	20.4	20.9	19.5
Fe_2O_3	7.60	11.3	6.76	8.87	10.0	12.5	9.38	6.16	7.96	7.09	4.64	9.90	12.9	5.78	11.8	13.0	8.88	9.82	11.8
MnO	0.14	0.10	0.18	0.19	0.14	0.14	0.10	0.07	0.11	0.12	0.09	0.11	0.15	0.09	0.15	0.17	0.13	0.15	0.19
MgO	7.52	9.38	11.8	8.42	8.50	7.46	7.20	9.83	17.3	9.77	8.46	13.3	9.62	7.12	7.28	8.70	11.0	8.84	8.54
CaO	7.28	6.74	6.96	5.82	5.42	10.1	9.01	5.96	11.9	8.02	11.3	7.54	10.3	9.76	7.65	8.06	4.92	6.03	4.85
Na_2O	3.56	3.58	3.01	3.06	3.99	3.02	3.74	3.86	1.18	2.67	3.14	2.78	3.08	3.76	1.69	2.54	1.6	1.73	0.87
K_2O	2.32	1.11	1.14	2.05	2.54	0.94	1.61	1.12	0.82	2.90	1.92	0.86	0.92	1.63	3.81	2.18	3.54	4.23	3.90
P_2O_5	0.12	0.18	0.25	0.23	0.22	0.04	0.01	0.02	0.01	0.02	0.02	0.02	0.02	0.02	n.d.	0.01	0.01	n.d.	0.19
L.O.I.	2.09	3.49	4.63	2.88	3.42	1.03	1.24	4.32	4.37	3.23	1.85	1.32	1.22	1.78	1.65	2.59	4.48	3.27	4.36
Total	100.03	100.26	100.00	99.96	99.91	100.16	100.07	99.95	100.22	100.08	100.08	100.11	100.27	100.09	100.01	100.01	100.09	99.61	99.93
mgV	69.0	65.1	65.8	68.1	65.8	57.3	63.3	79.2	83.1	75.6	80.4	75.1	62.6	73.5	58.4	60.1	73.8	67.2	56.4
Ni	67	32	14	11	47	24	84	75	388	72	96	202	136	108	46	36	103	57	21
Co	30	25	19	26	27	35	43	29	73	45	34	70	55	35	28	32	40	35	25
Cr	200	15	31	36	75	60	90	132	338	73	170	24	208	384	61	34	98	58	56
V	188	482	274	238	294	349	368	165	174	158	181	43	437	150	367	464	246	346	359
Cu	28	50	19	11	25	44	43	13	140	25	129	33	76	26	–	48	59	–	–
Zn	72	103	98	104	110	134	64	38	49	36	25	61	71	42	–	126	81	–	–
Ga	18	22	22	22	16	23	19	16	10	15	34	9	16	15	–	22	17	–	–
Rb	45	20	18	45	41	12	24	24	16	69	45	11	15	29	70	39	82	97	122
Sr	385	311	317	310	237	369	364	430	44	378	422	396	271	393	550	256	139	201	141
Ba	807	186	281	229	601	149	332	233	–	1366	286	160	175	467	–	422	413	413	–
Zr	38	48	31	43	93	25	19	23	44	24	22	(4)	34	26	–	18	19	15	38
Nb	5	9	6	7	9	(3)	n.d.	(3)	23	(5)	(3)	n.d.	n.d.	n.d.	n.d.	n.d.	n.d.	n.d.	n.d.
Y	13	32	20	20	37	26	7	10	(3)	8	10	n.d.	16	9	25	29	12	25	32
K/Rb	428	461	526	378	514	650	567	387	425	349	354	649	509	466	452	464	358	362	265

Tab. 7 REE analyses of selected mafic granulites. For sample reference see table 6.

	1 225C	2 C4	3 229E	4 235G	5 209B
La	5.48	10.0	2.72	3.02	1.16
Ce	11.9	28.9	8.02	6.81	2.08
Pr	1.72	4.87	1.58	0.96	0.27
Nd	8.10	25.1	9.64	4.24	1.18
Sm	2.15	6.47	3.43	1.23	0.25
Eu	0.86	1.72	1.14	0.65	0.24
Gd	2.19	5.75	3.53	1.46	0.28
Tb	0.34	0.94	0.64	0.25	0.04
Dy	2.13	5.53	3.69	1.61	0.23
Ho	0.47	1.20	0.83	0.29	0.06
Er	1.16	2.91	2.03	0.72	0.15
Yb	1.11	2.75	1.89	0.66	0.13
Lu	0.15	0.41	0.26	0.09	0.01
ΣREE	37.76	96.55	39.4	21.99	6.08
$(La/Yb)_N$	3.3	2.4	1.0	3.1	6.0

ments are probably controlled by the abundant amphibole (sample C4) and clinopyroxene + amphibole (sample 229E).

The positive correlation between mg-values and TiO_2, as well as the trend in the AFM diagram suggest that the protoliths of the mafic granulites crystallized from tholeiitic liquids, which is consistent with the observed iron enrichment trend of the pyroxenes (Fig. 3). The igneous protoliths were probably dominated by cumulus of pyroxenes and plagioclase (± olivine, ± amphibole), in agreement with the REE distribution.

The high variability of K_2O (0.82–4.23 wt%), Rb (11–142 ppm) and K/Rb ratios (182–650) is related to the amount of hydration and, in particular, to the replacement of plagioclase by white mica: the lowest values of K_2O, Rb and the highest K/Rb occur in the unaltered samples (e.g. 229E, 209B, 201A, Tab. 6), whereas the rocks with plagioclase completely converted into sericite (analyses 10, 17, 18, 19, Tab. 6) show high K_2O, Rb and the lowest K/Rb. Ba behaves coherently with Rb in most samples. Replacement of plagioclase should also produce CaO and Na_2O depletion which are more difficult to ascertain because these elements are also controlled by the modal proportions of amphibole and clinopyroxene. However, the most severely retrogressed samples, where plagioclase and clinopyroxene have been almost completely replaced by sericite and hornblende (analyses 17–19), show the lowest abundance of CaO (4.92–6.03 wt%) and Na_2O (0.90–1.69 wt%). Substantial chemical changes are therefore related to the retrograde metamorphic evolution.

Deformations and retrograde metamorphism

The retrograde metamorphic evolution of the mafic granulites can be traced through the compositional variations of the amphibole, which is very sensitive to the metamorphic conditions (e.g SPEAR, 1981; APTED and LIOU, 1983). The decreasing pargasite, tschermakite and Ti-Tschermakite substitutions, and the trend shown in the diagram Na/(Na + Ca) – Al/(Al + Si) of LAIRD and ALBEE (1981) (Fig. 4) mainly reflect retrograde metamorphic changes which are the reverse of the prograde reactions observed for regional metamorphic terrains of intermediate P/T gradients. The change in amphibole composition from hornblende to actinolite should indicate the transition between amphibolite- and greenschist-facies (e.g. LIOU et al., 1974; MARUYAMA et al., 1983). Although the existence of a miscibility gap between actinolite and hornblende is well assessed (see SMELIK et al., 1991 and references therein), the absence of textural and chemical evidence (exsolutions or compositional gap) suggests that the frequent coexistence of actinolite and hornblende is not the product of an equilibrium crystallization. The retrograde and frequently incomplete metamorphic changes suggest that coexisting hornblende and actinolite simply result from relatively fast cooling which hindered a complete compositional readjustement (GRAPES and GRAHAM, 1978).

The textural and mineralogical observations have allowed to recognize several deformation events in the granulitic rocks, although this reconstruction is obviously hampered by the lack of the original field relations.

High-T plastic deformations originated both in granulite- and upper amphibolite facies, possibly in discrete high-T shear zones. Weakly to strongly deformed rocks (mylonites and ultramylonites) have beeen recognized. In the mafic granulites syn-kinematic crystallization of clinopyroxene + Ti-rich pargasite occurs, whereas in the amphibolites shearing is related to the development of greenish-brown hastingsite + ilmenite after clinopyroxene + Ti-rich pargasite + green spinel. The Ti content of the amphibole coexisting with a Ti phase may be employed to calculate the temperature of amphibole formation (OTTEN, 1983). The hastingsitic amphiboles replacing Ti-rich pargasite in the mylonitic amphibolites give T between 580 °C and 700 °C, compatible with retrogression in the amphibolite facies.

The lower-T brittle deformations are related to development of (i) magnesio-hornblende (showing Ti content compatible with amphibolite-greenschist transition, RAASE, 1974) ± epidote

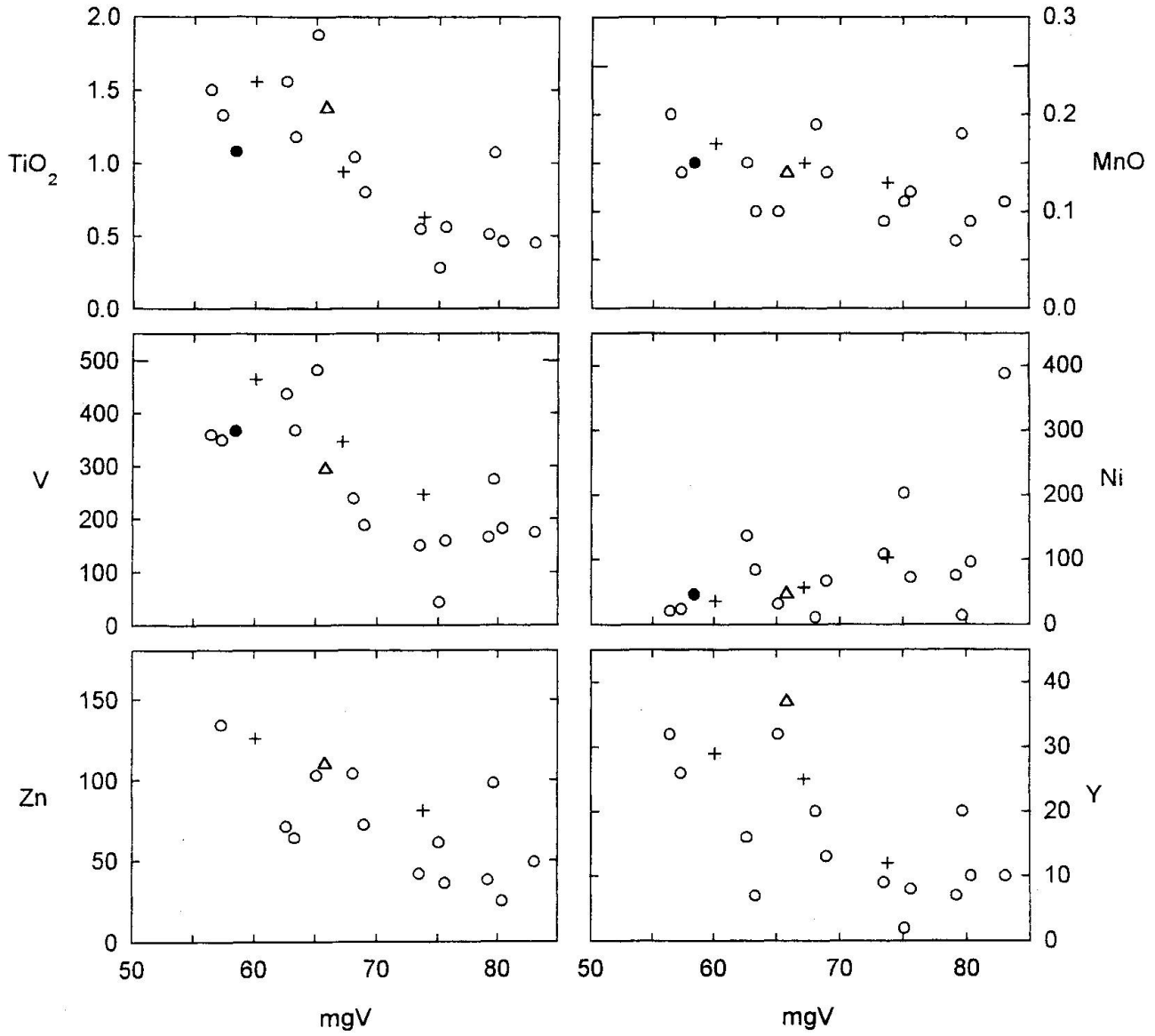

Fig. 5 Variation diagrams of TiO_2, MnO, V, Ni, Zn and Y plotted against mgV index (= 100 Mg/(Mg + Fe^{2+}); mgV calculated assuming $Fe_2O_3/FeO = 0.15$. Symbols: ○ = two–pyroxene granulites, ● = garnet granulite, △ = amphibole-rich pyroxene granulite, + = amphibolites. Oxides are in wt% and single elements in ppm.

and (ii) typical greenschist assemblages (actinolite-sericite-epidote-chlorite). The occurrence of brittle deformation at the depth required by the relatively high temperatures of the amphibolite-greenschist transition (T ~ 450 °C) can be attained only if confining P is low, i.e. $P_{fluid} \sim P_{tot}$ (BRODIE and RUTTER, 1985). The variable extent of deformations and retrograde effects and the chemical changes related to hydration, are identical to those reported for retrograde shear zones (BEACH, 1980; CORBETT and PHILIPS, 1981; SANDIFORD, 1984). In addition, the replacement of plagioclase by sericite is typical of low-T shear zones (BEACH, 1980).

In synthesis, many lines of evidence indicate that the complex history of retrogression and deformation of the granulitic rocks is related to involvement into high- and low-T shear zones during their progressive exhumation and emplacement to relatively shallow crustal levels.

The retrograde metamorphic imprint and related deformations must be largely pre-Alpine, since the orogenic metamorphism in the External Liguride Units did not exceed subgreenschist conditions. However, the lowest grade conditions recorded in the mafic granulites can be referred to the pumpellyite-actinolite facies (T = 250–350 °C, P > 1.5 kbar, FREY, 1987, Fig. 3.6) according to the occurrence of pumpellyite (+ chlorite, actinolite, sericite, albite) in some cataclastic rocks. The sub-

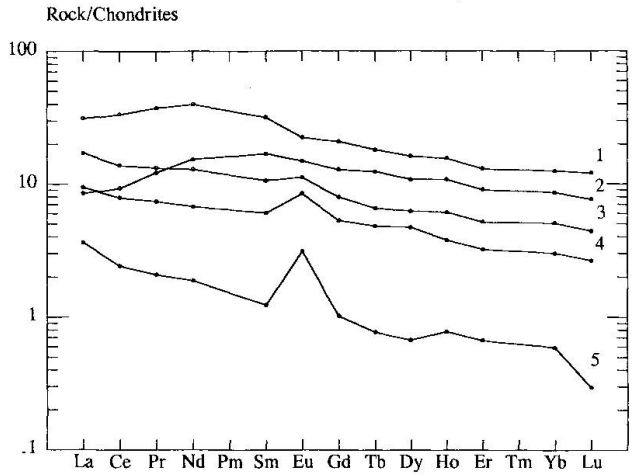

Fig. 6 Chondrite-normalized REE patterns of selected mafic granulites (normalizing values after EVENSEN et al., 1978). 1 = amphibole-rich pyroxene granulite (C4); 2 = spinel-rich mafic granulite (229E); 3 = opx-rich mafic granulite (225C); 4 = mafic gneiss (235G); 5 = symplectite-bearing granulite (209B).

greenschist assemblages could record a later, orogenic (eo-Alpine ?) event. The $^{40}Ar/^{39}Ar$ age (~ 80 Ma) obtained on the plagioclase of a mafic granulite (MELI et al., 1996) and similar fission-track ages recorded by the zircon of the felsic granulites (BALESTRIERI et al., in press) support this interpretation.

Comparison with the granulite-facies rocks from the Ivrea Zone

Palinspastic reconstructions of the Apennine chain indicate that the mafic granulites most probably came from the Adria continental margin (ABBATE and SAGRI, 1982; ELTER and MARRONI, 1991; ELTER, 1993). A comparison with the rocks belonging to the cross-section of deep crust exposed in the Ivrea Zone (which was part of the same continental block) leads to the following considerations:

(1) The mafic granulites from the northern Apennine have several mineralogical affinities with the Ivrea metabasic rocks and, in particular, with the Main Gabbro formation: (i) occurrence of two-pyroxene and garnet granulites, (ii) high Al_2O_3 content of the pyroxenes, (iii) composition of the high-grade amphiboles (CAPEDRI, 1971; SILLS, 1983), (iv) pyroxene-spinel coronas between olivine and plagioclase indicating isobaric cooling from igneous temperatures (SILLS, 1983). High- and low-T shear zones (possibly related to extensional deformations and thinning of the southern margin of the Tethys ocean) have been recognized in the Ivrea Zone (BRODIE and RUTTER, 1987; ZINGG et al., 1990) and a remarkable similarity can be observed between amphiboles from these shear zones and those from the present work (Fig. 4).

The Sm–Nd age obtained for a two-pyroxene granulite from the northern Apennine (291 ± 10 Ma with a initial Nd isotopic ratio corresponding to $\varepsilon_{Nd} = -4.4$, MELI et al., 1996) is most probably very close to the time of emplacement of the igneous protolith which was followed by recrystallization in granulite-facies conditions. Similar ages and initial Nd isotopic composition are reported in literature for the mafic rocks belonging to the Main Gabbro (PIN and SILLS, 1986; VOSHAGE et al., 1987; PIN, 1990). Moreover, the Ti-rich pargasitic amphibole of the same sample gives a younger $^{40}Ar/^{39}Ar$ age (228 ± 2 Ma, MELI et al., 1996) which record cooling below a blocking T of ~ 500 °C (HARRISON, 1981), probably related to uplift and extensional thinning of the crust. Similar, Permian to Triassic post-peak cooling ages have been determined in granulite- and amphibolite-facies rocks from the Ivrea zone (e.g. BRODIE et al., 1989; BORIANI and VILLA, 1995).

This brief comparison with the metabasic rocks from the Ivrea Zone suggests that the mafic granulites from the northern Apennine have coeval igneous protoliths derived from basaltic magmas which emplaced at comparable crustal levels and underwent a similar pre-Jurassic tectono-metamorphic history.

(2) The quartzo-feldspathic granulites and the charnockitic rocks are respectively similar to the sillimanite-free stronalites described by BERTOLANI and GARUTI (1970) and to the charnockites interlayered with metabasic rocks of the Ivrea Zone (SINIGOI et al., 1991).

Discussion and conclusions

The granulitic rocks enclosed in the ophiolitic chaotic complexes of Cretaceous age from the northern Apennine are predominantly composed of different varieties of two-pyroxene mafic granulites; minor garnet-bearing pyroxene granulites, pyroxenites and felsic granulites also occur. Amphibolites evidently formed through retrogression of mafic rocks are quite common.

The igneous protoliths of the mafic granulites are interpreted as originated in the deep crust through cumulus of pyroxenes and plagioclase (with minor olivine and amphibole) from variably evolved mafic liquids of likely tholeiitic affinity. Genetic relationships within the mafic granulites are strongly supported by the occurrence of tran-

sitional rock types and composite rocks together with remarkable mineralogic affinities and regular chemical variations. These rocks could have therefore originated in the same deep-seated intrusion. During post-magmatic cooling subsolidus re-equilibration occurred at intermediate pressure (~ 7–8 kbar) and high temperature (~ 800 °C), i.e. granulite-facies conditions. Many of the granulitic rocks have undergone a first retrograde event related to shear zones which can be placed both in granulite and upper amphibolite facies. Subsequently, a widespread lower-grade retrograde metamorphism coupled with brittle deformations and chemical changes caused by extensive hydration overprinted the high-T assemblages and deformations. The preserved disequilibrium assemblages record a wide range of metamorphic conditions from granulite-facies to subgreenschist assemblages. The retrograde metamorphic evolution and the deformations are most probably related to exhumation of the deep crust.

To attempt a tectonic interpretation of the granulitic rocks, the peculiar nature of the northern Apennine ophiolites and, in particular, of the ultramafic rocks associated with the granulites, must be taken into account. The peridotites of the External Liguride domain have geochemical and isotopic features typical of subcontinental mantle and record a history of subsolidus (non-adiabatic) uplift at progressively decreasing P-T conditions (RAMPONE et al., 1995). Their P-T evolution has been related to the early phases of the Tethyan rifting. According to the most recent petrological and tectonic interpretations, the opening of the Ligure-Piemontese Basin was related to a passive rifting mechanism along low-angle detachment faults with final tectonic denudation of the upper mantle in a pericontinental position (LEMOINE et al., 1987; PICCARDO et al., 1992; TROMMSDORRF et al., 1993; HOOGERDUJIN STRATING et al., 1993; FROITZHEIM and MANATSCHAL, 1996). Following this mechanism, mantle and deep crustal rocks are expected to have been exposed together close to the ocean-continent boundary (BOILLOT et al., 1980, 1995), although very few occurrences of lower crust together with exhumed subcontinental mantle have been reported up to now (see for example MÜNTENER and HERMANN, 1996).

It is therefore proposed that the retrograde path of the metamorphism related to development of high- and low-T shear zones and the association of blocks of lower continental crust with subcontinental mantle (External Liguride ultramafics) can be accounted for by exhumation through passive rifting. The slide blocks of peridotites, granulite-facies rocks and associated breccias can be interpreted as lithologies coming from the disgregation of peridotitic (subcontinental) mantle exposed close to the ocean-floor together with remnants of continental lower crust. Disgregation and enclosing into sedimentary mélanges occurred during the eo-Alpine (Upper Cretaceous) transpressive events which deformed the Eastern part of the Ligurian domain (ELTER and MARRONI, 1991).

Acknowledgements

The research has been supported by MURST 60% (L. Vernia, University of Parma) and MURST 40% (G. Zanzucchi, University of Parma). I am very grateful to L. Vernia, G. Zanzucchi and M. Zerbi for their stimulating suggestions. I wish also to thank Andreina Bonetta who provided many of the studied samples and Edvige Masini who drafted the maps. Electron microprobe and XRF analyses have been performed at the Istituto di Petrografia of the University of Parma. Careful reviews by K. Bucher, G. Piccardo and O. Müntener considerably improved the manuscript.

References

ABBATE, E. and SAGRI, M. (1982): Le unità torbiditiche dell'Appennino Settentrionale ed i margini continentali della Tetide. Mem. Soc. Geol. It. 24, 115–126.

ABBATE, E., BORTOLOTTI, V. and PRINCIPI, G. (1984): Pre-orogenic tectonics and metamorphism in Western Tethys ophiolites. Ofioliti 9, 245–278.

APTED, M.J. and LIOU, J.G. (1983): Phase relations among greenschist-epidote amphibolite and amphibolite in a basaltic system. Amer. J. Sci. 283, 328–354.

BALESTRIERI, M.L., BIGAZZI, G., MARRONI, M. and TRIBUZIO, R.: Quartzo-feldspathic granulites from External Liguride Units (northern Apennine): tectono-metamorphic evolution and thermochronological constraints from zircon fission-track data. C. R. Acad. Sci. Paris (in press)

BALLHAUS, C. and BERRY, R.F. (1991): Crystallisation pressure and cooling history of the Giles layered igneous complex, central Australia. J. Petrol. 32, 1–28.

BEACH, A. (1980): Retrogressive metamorphic processes in shear zones with special reference to the Lewisian complex. J. Struct. Geol. 2, 257–263.

BERTOLANI, M. and GARUTI, G. (1970): Aspetti petrografici della formazione basica Ivrea-Verbano in Val Sessera (Vercelli). Rend. Soc. It. Miner. Petrol. 26, 433–474.

BINGEN, B. DEMAIFFE, D. and DELHAL, J. (1984): Petrologic and geobarometric investigations in the Kasai gabbro-noritic complex and associated metadolerite dykes (Zaire). Bull. Mineral. 107, 665–682.

BOHLEN, S.R. (1987): Pressure-temperature-time paths and a tectonic model for the evolution of the granulites. J. Geol. 95, 617–632.

BOILLOT, G., GRIMAUD, S., MAUFFRET, A., MOUGENOT, D., KORNPROBST, J., MERGOIL-DANIEL, J. and TORRENT, G. (1980): Ocean-continent boundary off the Iberian margin: a serpentinite diapir west of the Galicia Bank. Earth Planet. Sci. Lett. 48, 23–34.

BOILLOT, G., AGRINIER, P., BESLIER, M.O., CORNEN, G., FROITZHEIM, N., GARDIEN, V., GIRARDEAU, J., GIL-

IBARGUCHI, JOSÉ-I., KORNPROBST, J., MOULLADE, M., SCHÄRER and VANNEY, J.-R. (1995): A lithospheric syn-rift shear zone at the ocean-continent transition: preliminary results of the Galineaute II cruise (Nautile dives on the Galicia Bank, Spain). C.R. Acad. Sci. Paris, 321, 1771–1778.

BORIANI, A. and VILLA, I.M. (1995): How to date regional metamorphism: Ivrea Zone-Serie dei Laghi (Southern Alps). Terra Abstr. 7, 270.

BRAGA, G., CASNEDI, R., GIAMMETTI, F., MARCHETTI, G. and ZERBI, M. (1975): Elementi di granuliti basiche in livelli clastici associati a masse ofiolitiche ultrafemiche del versante appenninico padano. Atti Ist. Geol. Univ. Pavia 25, 89–105.

BRODIE, K.H. and RUTTER, E.H. (1985). On the relationship between deformation and metamorphism with special reference to the behaviour of basic rocks. In: THOMPSON, A.B., RUBIE, D.C. (eds): Metamorphic reactions, Kinetics, Texture and Deformation. Adv. Phys. Geochem. 4, 138–179. Springer, Berlin.

BRODIE, K.H. and RUTTER, E.H. (1987): Deep crustal exstensional faulting in the Ivrea Zone of northern Italy. Tectonophysics 140, 193–212.

BRODIE, K.H., REX, D. and RUTTER, E.H. (1989): On the age of deep extensional faulting in the Ivrea zone, northern Italy. In: COWARD, M.P., DIETRICH, D. and PARK, R.G. (eds): Alpine Tectonics. Geol. Soc. Spec. Publ. 45, 201–210.

CAPEDRI, S. (1971): Sulle rocce della formazione basica Ivrea-Verbano. 2. Petrografia delle granuliti e rocce derivate affioranti nella Val Mastallone (Vercelli) e loro evoluzione petrogenetica. Mem. Soc. Geol. It. 10, 277–312.

C.N.R. Consiglio Nazionale delle Ricerche (1982): Carta strutturale dell'Appennino Settentrionale. S.E.L.C.A., Firenze.

CORBETT, G.J. and PHILIPS, G.N. (1981): Regional retrograde metamorphism of a high grade terrain: the Willyama Complex, Broken Hill, Australia. Lithos 14, 59–73.

CORTESOGNO, L. and LUCCHETTI, G. (1984): Il metamorfismo oceanico nei gabbri ofiolitici dell'Appennino Ligure: aspetti mineralogici e paragenetici. Rend. Soc. It. Mineral. Petrol. 38, 561–579.

COTTIN, J.Y. (1984): Les gabbros filonienes recoupant les lherzolites à spinelle et plagioclase du Bracco. Bull. Soc. Géol. France (7) 26, 935–944.

DAL PIAZ, G.V. (1993): Evolution of Austro-alpine and Upper Penninic basement in the North-Western Alps from Variscan convergence to post-Variscan extension. In: VON RAUMER, J.F. and NEUBAUER, F. (eds): Pre-Mesozoic Geology in the Alps, 327–344.

DAL PIAZ, G.V., DE VECCHI, G. and HUNZIKER, J.C. (1977): The austroalpine layered gabbros of the Matterhorn and Mt. Collon-Dents de Bertol. Schweiz. Mineral. Petrogr. Mitt., 57, 59–88.

DE WAARD, D. (1965): The occurrence of garnet in the granulite-facies terrane of the Adirondack Highlands. J. Petrol 6, 165–191.

EBERHARDT, P., FERRARA, G. and TONGIORGI, E. (1962): Détermination de l'âge des granites allochtones de l'Apennine septentrional. Bull. Soc. Geol. Fr. S. 7, 666–667.

ELLIS, D.J. and GREEN, D.H. (1985): Garnet-forming reactions in mafic granulites from Enderby Land, Antarctica – mineral assemblages and reactions. J. Petrol. 26, 633–662.

ELTER, P. (1993): Detritismo ofiolitico e subduzione: riflessioni sui rapporti tra Alpi e Appennino. Mem. Soc. Geol. It. 49, 205–215.

ELTER, P. and PERTUSATI, P.C. (1973): Considerazioni sul limite Alpi-Appennino e sulle loro relazioni con l'arco delle Alpi Occidentali. Mem. Soc. geol. It. 12, 359–375.

ELTER, P. and MARRONI, M. (1991): Le Unità Liguri dell'Appennino Settentrionale: sintesi dei dati e nuove interpretazioni. Mem. Descr. Carta Geol. d'It. 46, 121–138.

EVENSEN, N.M., HAMILTON, P.J. and O'NIONS, R.K. (1978): Rare earth abundances in chondritic meteorites. Geochim. Cosmochim. Acta 42, 1199–1212.

FAIRBAIRN, H.W. and HURLEY, P.M. (1971): Estimation of X-ray fluorescence and mass spectrometric analyses of Rb and Sr in some silicate standards. Geochim. Cosmochim. Acta 35, 149–156.

FREY, M. (1987): Low temperature metamorphism. Blackie, 351 pp.

FROITZHEIM, N. and MANATSCHAL, G. (1996): Kinematics of Jurassic rifting, mantle exhumation, and passive-margin formation in the Austroalpine and Penninic nappes (eastern Switzerland). Geol. Soc. Amer. Bull. 108, 1120–1133.

GASPARIK, T. (1987): Orthopyroxene thermobarometry in simple and complex systems. Contrib. Mineral. Petrol. 96, 357–370.

GLASSLEY, W. and SORENSEN, K. (1980): Constant P_s-T amphibolite to granulite-facies transition in Agto (West Greenland) metadolerites: implications and applications. J. Petrol. 21, 69–105.

GRAPES, R.H. and GRAHAM, C.M. (1978): The actinolite-hornblende series in metabasites and the so-called miscibility gap. Lithos 11, 85–97.

GREEN, D.H. and RINGWOOD, A.E. (1967): The genesis of basaltic magmas. Contrib. Mineral. Petrol. 15, 103–190.

GRIFFIN, W.L. and HEIER, K.S. (1973): Petrological implications of some corona structures. Lithos 6, 315–335.

GRIFFIN, W.L., WASS, S.Y. and HOLLIS, J.D. (1984): Ultramafic xenoliths from Bullenmerri and Gnotuk Maars, Victoria, Australia: petrology of a subcontinental crust-mantle transition. J. Petrol. 25, 53–87.

HARLEY, S.L. (1989): The origin of granulites: a metamorphic perspective. Geol. Mag. 126, 215–247.

HANSMANN, W., HERMANN, J., MÜNTENER, O. and TROMMSDORFF, V. (1995): U–Pb dating of single zircons from a gabbroic intrusion at the crust-mantle boundary (Val Malenco, Italy). Terra abstracts, supp. No. 1, 352.

HARRISON, T.M. (1981): Diffusion of ^{40}Ar in hornblende. Contrib. Mineral. Petrol. 78, 324–331.

HEBERT, R., SERRI, G. and HEKINIAN, R. (1989): Mineral chemistry of ultramafic tectonites and ultramafic to gabbroic cumulates from the major oceanic basins and Northern Apennine ophiolites (Italy) – a comparison. Chemical Geology 77, 183–207.

HERZBERG, C.T. (1978): Pyroxene geothermometry and geobarometry: experimental and thermodynamic evaluation of some subsolidus phase relations involving pyroxenes in the system CaO–MgO–Al_2O_3–SiO_2. Geochim. Cosmochim. Acta 42, 945–957.

HOLDAWAY, M.J. (1972): Thermal stability of Al–Fe epidote as a function of f_{O_2} and Fe content. Contrib. Mineral. Petrol. 37, 307–340.

HOOGERDUIJN STRATING, E.H., RAMPONE, E. PICCARDO, G.B., DRURY, M. and VISSERS, L.M. (1993): Subsolidus emplacement of matle peridotite during incipient oceanic rifting and opening of the Mesozoic Tethys (Voltri Massif, NW Italy). J. Petrol. 34, 901–927.

JOHNSON, C.A. and ESSENE, E.J. (1982): The formation of garnet in olivine-bearing metagabbros from the Adirondacks. Contrib. Mineral. Petrol. 81, 240–251.

KUSHIRO, I.K. and YODER, H.S. (1966): Anorthite-Forsterite and Anorthite-Enstatite reactions and their bearing on the basalt-eclogite transformation. J. Petrol. 7, 337–362.

LAIRD, J. (1988): Chlorites: metamorphic petrology. In: BAILEY, S.W. (ed.): Hydrous phyllosilicates. Reviews in Mineralogy 19, Mineralogical Society of America, Washington, 405–447.

LAIRD, J. and ALBEE, A.L. (1981): Pressure, temperature and time indicators in mafic schist: their application to reconstructing the polymetamorphic history of Vermont. Amer. J. Sci. 281, 127–175.

LEAKE, B.E. (1978): Nomenclature of amphiboles: Mineral. Mag. 42, 533–563.

LEMOINE, M., TRICART, P. and BOILLOT, G. (1987): Ultramafic and gabbroic ocean floor of the Ligurian Tethys (Alps, Corsica, Apennine): in search of a genetic model. Geology 15, 622–625.

LEONI, L. and SAITTA, M. (1976): X-ray fluorescence analysis of 29 trace elements in glass and rock standards. Rend. Soc. It. Miner. Petrol. 31, 479–510.

LEONI, L., MARRONI, M., SARTORI, F. and TAMPONI, M. (1996): Metamorphic grade in metapelites of the Internal Liguride units (northern Apennine, Italy). Eur. J. Mineral., 8, 35–50.

LINDSLEY, D.H. (1983): Pyroxene thermometry. Amer. Mineral 68, 477–493.

LIOU, J.G., KUNIYOSHI, S. and ITO, K. (1974): Experimental studies of the phase relations between greenschist and amphibolite in a basaltic system. Amer. J. Sci. 274, 613–632.

LOOCK, G. STOSCH, H.G. and SECK, H.A. (1990): Granulite facies lower crustal xenoliths from the Eifel, West Germany: petrological and geochemical aspects. Contrib. Mineral. Petrol. 105, 25–41.

MALL, A.P. and SHARMA, R.S. (1988): Coronas in olivine metagabbros from the Proterozoic Chotanagpur terrain at Mathurapur, Bihar, India. Lithos 21, 291–300.

MANNA, S.S. and SEN, S.K. (1974): Origin of garnet in the basic granulites around Saltora, W. Bengal, India. Contrib. Mineral. Petrol. 44, 195–218.

MARRONI, M. (1994): Deformational path of the Internal Liguride units (northern Apennine, Italy): record of shallow-level underplating in the Alpine accretionary wedge. Mem. Soc. geol. It. 48, 179–194.

MARRONI, M. and TRIBUZIO, R. (1996): Gabbro-derived granulites from External Liguride units (northern Apennine, Italy): implications for the rifting processes in the western Tethys. Geol. Rundsch. 85, 239–249.

MARUYAMA, S., SUZUKI, K. and LIOU, J.G. (1983): Greenschist-amphibolite transition equilibria at low pressures. J. Petrol. 24, 583–604.

MELI, S., MONTANINI, A., THONI, M. and FRANK, W. (1996): Age of mafic granulite blocks from the External Liguride Units (northern Apennine, Italy). Mem. Sci. Geol. Padova, 48, 65–72.

MERLA, G. (1933): I graniti della formazione ofiolitica appenninica. Bollettino del R. Ufficio Geologico d'Italia 58, 5–115.

MEVEL, C., CABY, R. and KIENAST, J.R. (1978): Amphibolite-facies conditions in the oceanic crust: example of amphibolitized flaser-gabbro and amphibolite from the Chenaillet ophiolite massif (Hautes Alpes, France). Earth Planet. Sci. Lett. 39, 98–108.

MOLLI, G. (1994): Microstructural features of high temperature shear zones in gabbros of the northern Apennine ophiolites. J. Struct. Geol. 16, 1535–1541.

MOLLI, G. (1996): Pre-orogenic tectonic framework of the northern Apennine ophiolites. Eclogae geol. Helv. 89, 163–180.

MONTANINI, A., MOLLI, G. and MELI, S. (1995): Continental crust rocks in the External Liguride Units of the northern Apennine (Italy): petrological, radiometric and structural data and their interpretation. In: Proceedings of the International Ophiolite Symposium, Pavia, Italy, 93–94.

MÜNTENER, O., HERMANN, J., PUSCHNIG, A.R., TROMMSDORFF, V. and PICCARDO, G.B. (1995): Sea floor emplacement of a fossil crust-mantle section and MORB intrusions into subcontinental mantle at the Adriatic passive continental margin (Malenco-Forno nappe/Switzerland, N-Italy). In: Proceedings of the IOS (International Ophiolite Symposium, Pavia, Italy), 96–97.

MÜNTENER, O. and HERMANN, J. (1996): The Val Malenco lower crust-upper mantle complex and its field relations (Italian Alps). Schweiz. Mineral. Petrogr. Mitt., 475–500.

NAYLOR, M. (1982): The Casanova complex of the northern Apennine: a mélange formed on a distal passive continental margin. J. Struct. Geol. 4, 1–18.

OLIVER, G.J.H. (1978): Ilmenite-magnetite geothermometry and oxygen barometry in granulite and amphibolite facies gneisses from Doubtful Sound, Fiordland, New Zealand. Lithos 11, 147–153.

OTTEN, M.T. (1983): The origin of brown hornblende in the Artfjället gabbro and dolerites. Contrib. Mineral. Petrol. 86, 189–199.

PICCARDO, G.B., RAMPONE, E. and VANNUCCI, R. (1992): Ligurian peridotites and ophiolites: from rift to ocean formation in the Jurassic Ligure-Piemontese basin. Acta Vulcanol. 2, 313–325.

PIN, C. (1986): Datation U/Pb sur zircons à 285 Ma du complexe gabbro-dioritique du Val Sesia-Val Mastallone et âge tardi-hercynien du métamorphisme granulitique de la zone Ivrea-Verbano (Italie). C.R. Acad. Sci. Paris, 303, 827–830.

PIN, C. (1990): Evolution of the lower crust in the Ivrea Zone: a model based on isotopic and geochemical data. In: VIELZEUF, D. and VIDAL, PH. (eds): Granulites and crustal evolution. NATO ASI Series, Kluwer, Dordrecht, 87–110.

PIN, C. and SILLS, J.D. (1986): Petrogenesis of layered gabbros and ultramafic rocks from Val Sesia, the Ivrea Zone, NW Italy: trace element and isotope geochemistry. In: DAWSON, J.B., CARSWELL, D.A., HALL, J. and WEDEPOHL, K.H. (eds): The nature of the lower continental crust. Geological Society Special Publication. Blackwell, Oxford, 231–249.

RAASE, P. (1974): Al and Ti contents of hornblende, indicators of pressure and temperature of regional metamorphism. Contrib. Mineral. Petrol. 45, 231–236.

RAASE, P., RAITH, M., ACKERMAND, D. and LAL, R.K. (1986): Progressive metamorphism of mafic rocks from greenschist to granulite facies in the Dharwar craton of South India. J. Geol. 94, 261–282.

RAMPONE, E., HOFFMANN, A.W., PICCARDO, G.B., VANNUCCI, R., BOTTAZZI, P. and OTTOLINI, L. (1995): Petrology, mineral and isotope geochemistry of the External Liguride peridotites (northern Apennine, Italy). J. Petrol. 36, 81–105.

RAMPONE, E., HOFFMANN, A.W., PICCARDO, G.B., VANNUCCI, R., BOTTAZZI, P. and OTTOLINI, L. (1996): Trace element and isotope geochemistry of depleted peridotites from a N-MORB type ophiolite (Internal Liguride, N. Italy). Contrib. Mineral. Petrol. 123, 61–76.

RIETMEJIER, F.J.M. (1983): Chemical distinction between igneous and metamorphic orthopyroxenes, especially those coexisting with Ca-rich clinopyroxene: a re-evaluation. Mineral. Mag. 47, 143–151.

ROCK, N.M.S. (1990): The International Mineralogical Association (IMA/CNMMN) pyroxene nomenclature scheme: computerization and its consequences. Mineral. Petrol. 43, 99–119.

SANDIFORD, M. (1984): The origin of retrograde shear zones in the Napier Complex: implications for the tectonic evolution of Enderby Land, Antarctica. J. Struct. Geol. 7, 477–488.

SEYLER, M. and BONATTI, E. (1988): Petrology of a gneiss-amphibolite lower crustal unit from the Zabargad island, Red Sea. Tectonophysics 150, 177–207.

SILLS, J.D. (1983): Granulite facies metamorphism in the Ivrea Zone, northern Italy. Schweiz. Mineral. Petrogr. Mitt. 64, 169–191.

SINIGOI, S., ANTONINI, P., DEMARCHI, G., LONGINELLI, A., MAZZUCCHELLI, M., NEGRINI, L. and RIVALENTI, G. (1991): Interactions of mantle and crustal magmas in the southern part of the Ivrea Zone. Contrib. Mineral. Petrol. 108, 385–395.

SMELIK, E.A., NYMAN, M.W. and VEBLEN, D.R. (1991): Pervasive exsolution within the calcic amphibole series: TEM evidence for a miscibility gap between actinolite and hornblende in natural samples. Amer. Mineral. 76, 1184–1204.

SPEAR, F.S. (1981): An experimental study of hornblende stability and compositional variability in amphibolite. Amer. J. Sci. 281, 697–734.

SPEAR, F.S. and KIMBALL, K.L. (1984): RECAMP – A Fortran IV program for estimating Fe^{3+} contents in amphiboles. Computers and Geosciences 10, 317–325.

SPENCER, K.J. and LINDSLEY, D.H. (1981): A solution model for coexisting iron-titanium oxides. Amer. Mineral. 66, 1189–1201.

TROMMSDORFF, V., PICCARDO, G.B. and MONTRASIO, A. (1993): From magmatism through metamorphism to sea floor emplacement of subcontinental Adria lithosphere during pre-Alpine rifting (Malenco, Italy). Schweiz. Mineral. Petrogr. Mitt. 73, 191–203.

VENTURELLI, G. and FREY, M. (1977): Anchizone metamorphism in sedimentary sequences of the northern Apennine (preliminary results). Rend. Soc. It. Miner. Petrol. 33, 109–123.

VENTURELLI, G., CAPEDRI, R.S., THORPE, R.S. and POTTS, P.J. (1981): Rare earth and trace elements characteristic of ophiolitic metabasalts from the Alpine-Appenine belt. Earth Planet. Sci. Lett. 53, 109–123.

VOSHAGE, H., HUNZIKER, J.C., HOFMANN, A.W. and ZINGG, A. (1987): A Nd and Sr isotopic study of the Ivrea Zone, Southern Alps, N-Italy. Contrib. Mineral. Petrol. 97, 31–49.

WELLS, P.R.A. (1977): Pyroxene thermometry in simple and complex systems. Contrib. Mineral. Petrol. 62, 129–139.

WERNICKE, B. (1985): Uniform sense of simple shear of the continental lithosphere. Can. J. Earth Sci. 22, 108–125.

ZANZUCCHI, G. (1988): Ipotesi sulla posizione paleogeografica delle "Liguridi Esterne" cretacico-eoceniche nell'Appennino Settentrionale. Atti Tic. Sci. Terra 31, 327–339.

ZINGG, A., HANDY, M.R., HUNZIKER, J.C. and SCHMID, S.M. (1990): Tectonometamorphic history of the Ivrea Zone and its relationship to the crustal evolution of the Southern Alps. Tectonophysics 182, 169–192.

Manuscript received April 17, 1996; revised manuscript accepted December 11, 1996.